Inference of Intensity-Based Models for Load-Sharing Systems With Damage Accumulation

Christine H. Müller and Renate Meyer

***Abstract*—To model damage accumulation for load-sharing systems, two models given by intensity functions of self-exciting point processes are proposed: a model with additive damage accumulation and a model with multiplicative damage accumulation. Both models include the model without damage accumulation as a special case. For both models, the likelihood functions are derived and maximum likelihood estimators and likelihood ratio tests are given in a scale-invariant version and a scale-dependent version. Furthermore, a Bayesian approach using Markov chain Monte Carlo methods for posterior computation is provided. The frequentist and Bayesian methods are applied to a data set of failures of tension wires of concrete beams where a significant damage accumulation effect is confirmed by both additive and multiplicative damage accumulation models. This is all the more remarkable as a simulation study indicates that the tests for an existing damage accumulation effect are rather conservative. Moreover, prediction intervals for the failure times of the tension wires in a new experiment are given, which improve former prediction intervals derived without damage accumulation. The simulation study considers a scenario with a fixed time horizon and one with fixed numbers of failed components of the systems.**

***Index Terms*—Bayesian inference, confidence sets, credible sets, deviance information criterion, Gibbs sampler, likelihood ratio test, prediction intervals, self-exciting point process.**

NOMENCLATURE

Acronyms

W	Model without damage accumulation.
M	Model with multiplicative damage accumulation.
A	Model with additive damage accumulation.
$\mathcal{M}$	$\mathcal{M} = W$, $\mathcal{M} = M$, or $\mathcal{M} = A$.
ML	Maximum likelihood.

Notation

j	Number of system ($j = 0, 1, \ldots, J$).
$j = 0$	A new system.
s_j	Initial stress in system j.
$\mathcal{K}_j$	Number of components in system j.
I_j	Number of observed failures in system j.
τ_j	End of observation time in system j.
τ	$\tau = \frac{1}{J}\sum_{j=1}^{J}\tau_j$ or $\tau = \tau_\star$ with given $\tau_\star$.
I_c	Critical number of failures.
$\mathcal{N}_j(t)_{t\le\tau_j}$	Point process of failures in system j.
$N_j(t)_{t\le\tau_j}$	Realization of $\mathcal{N}_j(t)_{t\le\tau_j}$.
$T_{i,j}$	Time of ith failure in system j, $T_{0,j} := 0$.
$t_{i,j}$	Realization of T_{ij}.
W_{ij}	$W_{ij} := T_{i,j} - T_{i-1,j}$, $i = 1, \ldots, I_j$.
$W_{(I_j+1)j}$	$W_{(I_j+1)j} := \tau_j - W_{I_j j}$.
a_{ij}	Load-sharing stress at t_{ij}.
$a_j(t)$	Load-sharing stress at time t.
$C_j(i)$	Cumulated stress at t_{ij}.
$A_j(t)$	Cumulated stress at time t.
$\lambda_j(t)$	Intensity function at t with $\lambda_j^{\mathcal{M}}(t)$ for model $\mathcal{M} =$ *W*, *M*, *A*.
$\Lambda_j(t)$	Cumulative intensity function at t with $\Lambda_j^{\mathcal{M}}(t)$ for model $\mathcal{M} = W, M, A$.
θ	Unknown parameter vector.
$\widehat{\theta}$	Estimator of θ.
$L(\theta)$	Likelihood function at θ with $L_{\mathcal{M}}(\theta)$ for model $\mathcal{M}$ = *W*, *M*, *A*.

Manuscript received June 4, 2021; revised September 30, 2021; accepted December 28, 2021. This work was supported in part by the Collaborative Research Center "Statistical Modelling of Nonlinear Dynamic Processes" (SFB 823, B5) of the German Research Foundation (DFG), and in part by the Distinguished Visitor Award of the University of Auckland that facilitated a visit of Christine H. Müller to the University of Auckland in 2019. The work of Renate Meyer was supported in part by the James Cook Fellowship JCF-UOA1801 administered by the Royal Society Te Aparangi. Associate Editor: Yiming Deng. *(Corresponding author: Christine H. Müller.)*

Christine H. Müller is with the Department of Statistics, TU Dortmund University, 44227 Dortmund, Germany (e-mail: cmueller@statistik.tu-dortmund.de).

Renate Meyer is with the Department of Statistics, The University of Auckland, Auckland 1142, New Zealand (e-mail: renate.meyer@auckland.ac.nz).

Color versions of one or more figures in this article are available at https://doi.org/10.1109/TR.2022.3140483.

Digital Object Identifier 10.1109/TR.2022.3140483

I. Introduction

CONSIDER J systems, each with $\mathcal{K}_j$, $j = 1, \ldots, J$, parallel components which fail successively due to a stress s_j which may be different for the J systems. In a load-sharing system, the stress is redistributed to the surviving components of the system after a component of the system has failed. This type of behavior occurs, for example, in systems of electrical components, fiber bundles, or lumber constructions; see also [1] for other examples. In particular, we are interested in the failure times of concrete beams each consisting of $\mathcal{K}_j = 35$ tension wires. The tension wires break successively due to their cyclic load. The exact time points of the breaks are determined by acoustic measurements.

The study of load-sharing systems goes back to [2]–[5] who derived reliability properties. These studies are ongoing; see, e.g., [6]–[11].

Statistical inference for load-sharing systems has mainly been developed over the last 20 years. Many authors such as [1], [12]–[16] have studied models where the number of unknown parameters coincides with the number of failures observed in the system. These approaches can only be applied if the number of

components of the system is not too high. The authors in[17]–[19] reduce the number of unknown parameter to one or two parameters using special link functions.

In all these models, the stress on the remaining components is modeled as a function of the *number* of failed components. The *duration* of the load-shared stress is not included in the models. However, it is very likely that the failure risk of the remaining components does not only depend on the number of remaining components but also on how long the remaining components were exposed to the redistributed stress. Degradation processes will often lead to a damage accumulation which increases the risk of failure continuously between successive failures.

There are several approaches to model and analyze damage accumulation and degradation by continuously increasing stochastic processes such as those of [20]–[25]. These degradation processes can also be linked to different stress levels for accelerated life testing as was done, for example, by [26]. In step-stress accelerated degradation testing as in [27] and [28], the stress is increased stepwise during the degradation process. Most of these approaches assume that the stepwise increase of the stress is given by the experimenter at predefined time points and the effect of increased stress is modeled by the cumulative distribution function in so-called cumulative exposure models originally proposed by [29].

It is also possible to use the cumulative exposure model when the stepwise increase of the stress is caused by failing components as in [16]. Then the cumulative distribution functions are conditional cumulative distribution functions depending on the past failure times. However, the approach of [16] results in failure risk (hazard) functions which depend only on the number of failed components which can be seen from the derived hazard functions in [30] for a general class of distributions. Moreover, the hazard functions are constant between failure time points if the exponential distribution is used. The combination of the cumulative exposure model with a degradation process as in [27] and [28] also provides no failure risk depending on the history of failures since the degradation process depends additionally only on the cumulated time. This is similar to the approach of [1] and [31] where a fixed failure rate function is multiplied by load-sharing effects. Similarly, the authors of [32] add a simple load-sharing effect to a Wiener degradation process and estimate only the parameters of the Wiener process.

Hence, all these models for degradation and load-sharing assume that the actual failure risk depends only on the current number of failed components and the cumulated time, but the failure risk is independent of the damage accumulation in the past. This means that these models do not model the history of damage accumulation even though this history may have an important effect. For example, the failure risk of the remaining components of a system after the failure of the second component may not only depend on the failure time of the second component but also on the time of the first failure. If the first failure happens very early, then the remaining components are exposed to higher stress for a longer time than in the case where the first failure appears shortly before the second failure. Hence, the failure risk function should depend on the time intervals between past failures.

Here, we propose an alternative approach by considering the failure times as realizations of a point process. The interarrival times of the point process are the times between successive failures in a system. For load-sharing models, many authors such as in [12], [14], [16], and [33] assume that these interarrival times have an exponential distribution which depends only on the number of failures observed before. This assumption means that the corresponding point process is a birth process as considered in [34, pp. 95–96] and in [35, pp. 21, 95]. A birth process has a constant intensity rate (hazard rate) between the events (failures). To incorporate the potential damage accumulation, we assume an increasing intensity rate between the failures where the increase depends on all past interarrival times, i.e., the history of damage accumulation. This yields a so-called self-exciting point process with interarrival times that are not exponentially distributed; see, e.g., [34, p. 287]. We present an additive and a multiplicative model to include the past interarrival times and consider two scenarios: systems observed up to a given finite time horizon and systems observed up to a given number of failures. The scenario with given number of failures is realistic for systems with short failure times, while a fixed time horizon is often used in experiments with long failure times. The scenario of a fixed time horizon provides censored observations which we incorporate in our analysis.

In Section II-A, the intensity functions of the load-sharing models with additive and multiplicative damage accumulation are derived. These intensity functions are given in a scale-dependent and a scale-invariant version. Section II-B presents the likelihood functions for these models and Section II-C demonstrates how to simulate the damage accumulation processes. Section III-A discusses briefly the calculation of the maximum likelihood (ML) estimators and provides two types of likelihood ratio tests: one for testing for an existing damage accumulation effect and one for testing for a given parameter vector. Thereby, the second test can be used to provide confidence sets and prediction intervals as in [19]. An alternative Bayesian approach to estimating the parameters of these models and to calculating prediction intervals is outlined in Section III-B. In Section IV, we apply the methods to our data from the experiments with concrete beams. It turns out that the damage accumulation effect is significant in both load-sharing models with damage accumulation. This holds although the likelihood ratio test for this effect is rather conservative for finite samples as is shown by the simulations in Section V. This significance of the damage accumulation effect is furthermore corroborated by the Bayesian model comparisons. Moreover, the calculated prediction intervals for a new experiment in Section IV-C improve the results of [19] using a model without damage accumulation. Finally, Section VI provides a discussion of the results. All proofs are given in the Appendix.

II. Load-Sharing Models With and Without Damage Accumulation

Assume that there are J stochastically independent systems where the jth system has $\mathcal{K}_j$ components. The systems are exposed to different initial stresses s_j and are observed up to

different time points τ_j for $j = 1, \ldots, J$. The total number of observed failed components up to τ_j is denoted by I_j. Clearly, $I_j \leq \mathcal{K}_j$. Then the failure times of the components of the jth system $0 < t_{1,j} < \cdots < t_{I_j,j}$ are realizations of $T_{1,j} < \cdots < T_{I_j,j}$ and $N_j(t)_{t \leq \tau_j}$ with

$$N_j(t) := \sum_{i=1}^{\mathcal{K}_j} \mathbb{1}_{(0,t]}(t_{i,j})$$

is the realization of the corresponding counting process $\mathcal{N}_j(t)_{t \leq \tau_j}$ over $[0, \tau_j]$ with $N_j(\tau_j) = I_j$. A counting process $\mathcal{N}_j(t)_{t \leq \tau_j}$ is also called a point process according to [36]. Set $T_{0,j} := t_{0,j} := 0$. If $N_j(\tau_j) = \mathcal{K}_j$, then all of the $\mathcal{K}_j$ components have failed, i.e., $I_j = \mathcal{K}_j$, and we set $\tau_j := t_{\mathcal{K}_j,j} = t_{I_j,j}$ since it is clear that the experiment stops at $t_{I_j,j}$ in this case. The point processes $\mathcal{N}_j(t)_{t \leq \tau_j}$ are stochastically independent for $j = 1, \ldots, J$.

A. Intensity Functions

Point processes $\mathcal{N}_j(t)_{t \leq \tau_j}$ are completely determined by their intensity functions $\lambda_j(t)_{t \leq \tau_j}$ which are stochastic processes depending on past events. Especially, it holds that $E[\mathcal{N}_j(t)] = E[\int_0^t \lambda_j(t)dt]$ and $\lambda_j(t)dt \approx E[\mathcal{N}_j(dt)|\mathcal{H}_{j,t-}]$ where $\mathcal{H}_{j,t-}$ is the σ-algebra of events at times up to but not including t, see, e.g., [36, p. 232, Lemma 7.2.V on p. 241] or [37, pp. 51, 66, 73]. This means that $\lambda_j(t)$ describes the risk that a component of the system j fails at time t if the previous failures before t are given.

If the systems are load-sharing systems without damage accumulation, the following left-continuous conditional intensity function for the jth system with $\mathcal{K}_j$ components and initial stress s_j is a sensible choice

$$\lambda_j(t) = b_\theta\left(a_j(t)\right) \tag{1}$$

where b_θ is an increasing function depending on a parameter vector θ and a_j is an increasing function of the stress s_j and the number $N_j(t-) := \sum_{i=1}^{\mathcal{K}_j} \mathbb{1}_{(0,t)}(t_{i,j})$ of failures before t. $a_j(t)$ provides the actual stress for the components at time t. Note that an increasing function b_θ only makes sense for systems that are weakened by component failures. There exists systems, for example, in software reliability, where this might be not the case.

In particular, we set

$$a_{ij} := a_j(t) \quad \text{if} \quad N_j(t-) = i - 1.$$

An example of $a_j(t)$ and a_{ij} is given by

$$a_j(t) = \frac{s_j}{\mathcal{K}_j - N_j(t-)} \quad \text{and}$$

$$a_{ij} = \frac{s_j}{\mathcal{K}_j - N_j(t-)} = \frac{s_j}{\mathcal{K}_j - (i-1)}. \tag{2}$$

This provides the so-called "equal load-sharing model." It means that for t with $N_j(t-) = 0$, i.e., no failure is observed before time t, we get $a_j(t) = \frac{s_j}{\mathcal{K}_j}$, i.e., the initial stress is distributed equally over the $\mathcal{K}_j$ components. Moreover, for t with $N_j(t-) = \frac{\mathcal{K}_j}{2}$, we get $a_j(t) = \frac{2\,s_j}{\mathcal{K}_j}$. Hence, the stress doubles for each of the remaining components after half of the components have failed.

A reasonable link function b_θ between actual stress and failure time is given by the power law model of Basquin [38] who provided a link between stress x and lifetime in the form

$$b_\theta(x) := \exp(-\theta_1 + \theta_2 \ln(x)) = \exp(-\theta_1) x^{\theta_2} \tag{3}$$

with $\theta_1 \in \mathbb{R}$ and $\theta_2 \in [0, \infty)$.

In particular, model (1) implies that the conditional intensities between events are constant. Hence, the interarrival times (waiting times) $W_{ij} := T_{i,j} - T_{i-1,j}$ have an exponential distribution with rate parameter $b_\theta(a_{ij})$. Using the power law of Basquin, it holds then

$$\ln(E(W_{ij})) = \theta_1 - \theta_2 \ln(a_{ij})$$

so that the time between successive failures decreases with increased actual stress a_{ij}. In the following, we exclusively use the Basquin link (3) so that the intensity function of a model without damage accumulation is given by

$$\tilde{\lambda}_j^W(t) := \exp(-\theta_1) a_j(t)^{\theta_2}.$$

Since the main aim is to extend this model to a model with damage accumulation, the cumulative risk $\Lambda_j(t) := \int_0^t \lambda_j(x)\,dx$ is of high importance. To get a cumulative risk that does not depend on the time scale of t (measured, e.g., in seconds, minutes, hours, days, and years), it is appropriate to consider

$$\lambda_j^W(t) := \frac{1}{\tau} \exp(-\theta_1) a_j(t)^{\theta_2} \tag{4}$$

for the model without damage accumulation (also called model *W* here).

The value τ can be chosen automatically as mean time horizon

$$\frac{1}{J} \sum_{j=1}^{J} \tau_j$$

or manually as a given value $\tau_\star$. The use of $\tau = \frac{1}{J}\sum_{j=1}^{J} \tau_j$ leads automatically to time scale-invariant estimators and cumulative risks. However, simulation studies for this choice of τ are more difficult as will become apparent later. Moreover, this choice is only possible when the time horizons are specified in advance by the experimenter. However, time horizons are not fixed if the experiment is allowed to continue until a certain amount of failures have occurred. Then $\frac{1}{J}\sum_{j=1}^{J} \tau_j$ depends on the stochastic processes and will influence the behavior of the statistical methods. To accommodate this sampling situation, we introduced the option of choosing a fixed value τ_* for τ where τ_* should be in accordance with the respective unit of time measurements. Then the cumulative risks and estimates depend on this $\tau_\star$. However, if the time scale and $\tau_\star$ are changed concordantly (e.g., the time scale is changed from seconds to minutes and $\tau_\star$ is changed to $\tau_\star/60$), then the cumulative risks and the estimates remain unchanged.

To extend this model without damage accumulation to a load-sharing model with damage accumulation, first note that

$$A_j(t) := \int_0^t a_j(x)dx$$

$$= \left(a_j(t) \left(t - \sum_{k=1}^{N_j(t-)} W_{kj} \right) + \sum_{k=1}^{N_j(t-)} a_{kj} W_{kj} \right)$$

accumulates the stress $a_j(x)$ until time t in the sense of load sharing. In particular, $A_j(t)$ takes into account how long the stress was distributed over the remaining components. Again, it is reasonable to divide $A_j(t)$ by τ to adjust for the time scaling.

One could use $A_j(t)$ inside the Basquin link. However, then the pure load-sharing model given by (4) would not be a special case. Therefore, the following two models are considered as genuine extensions of the load-sharing model (4).

Model *M*: load sharing with multiplicative damage accumulation given by

$$\lambda_j^M(t) := \frac{1}{\tau} \exp(-\theta_1) a_j(t)^{\theta_2} \left(\frac{1}{\tau} A_j(t) \right)^{\theta_3} \tag{5}$$

and

Model *A*: load sharing with additive damage accumulation given by

$$\lambda_j^A(t) := \frac{1}{\tau} \exp(-\theta_1) \left(a_j(t) + \theta_3 \frac{1}{\tau} A_j(t) \right)^{\theta_2}. \tag{6}$$

In both models, the pure load-sharing model (4) is obtained by setting $\theta_3 = 0$. Note also that the second τ in (5) and (6) especially allows to avoid too small or too large effects of $A_j(t)$ for some time scales and thus can avoid numerical problems. As is shown later, these numerical problems can be serious, in particular, for model *A* if τ is chosen inappropriately for the time scale.

B. Likelihood Functions

Although not a proper waiting/interarrival time, setting $W_{(I_j+1)j} := \tau_j - t_{I_j,j}$, $j = 1, \ldots, J$, allows to define the cumulative stress

$$C_j(0) := 0, \quad C_j(i) := \sum_{k=1}^{i} a_{kj} W_{kj}, \quad i = 1, \ldots, I_j + 1 \tag{7}$$

for $j = 1, \ldots, J$. In particular, we set $a_{(\mathcal{K}_j+1)j} := 0$ if $I_j = \mathcal{K}_j$, i.e., if all components have failed.

Theorem II.1: Let L_M and L_A denote the likelihood function for the load-sharing model with multiplicative and additive damage accumulation given by (5) and (6), respectively. Then the log-likelihood functions are given by

$$\begin{aligned}
&\ln(L_M((\theta_1, \theta_2, \theta_3)^\top)) \\
&= \sum_{j=1}^{J} \left\{ \sum_{i=1}^{I_j} [-\theta_1 + \theta_2 \ln(a_{ij}) \right. \\
&\quad \left. + \theta_3 \ln\left(\frac{1}{\tau} C_j(i) \right) - \ln(\tau) \right] \\
&\quad - \frac{\exp(-\theta_1)}{\theta_3 + 1} \left[\sum_{i=1}^{I_j+1} a_{ij}^{\theta_2 - 1} \left(\left(\frac{1}{\tau} C_j(i) \right)^{\theta_3+1} \right. \right. \\
&\quad \left. \left. - \left(\frac{1}{\tau} C_j(i-1) \right)^{\theta_3+1} \right) \right] \right\}
\end{aligned} \tag{8}$$

and

$$\begin{aligned}
&\ln(L_A((\theta_1, \theta_2, \theta_3)^\top)) \\
&= \sum_{j=1}^{J} \left\{ \sum_{i=1}^{I_j} \left[-\theta_1 + \theta_2 \ln\left(a_{ij} + \theta_3 \frac{1}{\tau} C_j(i) \right) - \ln(\tau) \right] \right. \\
&\quad - \frac{\exp(-\theta_1)}{\theta_3(\theta_2 + 1)} \left[\sum_{i=1}^{I_j+1} \frac{1}{a_{ij}} \left(\left(a_{ij} + \theta_3 \frac{1}{\tau} C_j(i) \right)^{\theta_2+1} \right. \right. \\
&\quad \left. \left. \left. - \left(a_{ij} + \theta_3 \frac{1}{\tau} C_j(i-1) \right)^{\theta_2+1} \right) \right] \right\}.
\end{aligned} \tag{9}$$

Let L_W be the likelihood function of the load-sharing model without damage accumulation given by (4). Then, L_W can be obtained from the likelihood function of the load-sharing model with multiplicative damage accumulation by setting $\theta_3 = 0$. Setting $\theta_3 = 0$ is not possible for the likelihood function of the load-sharing model with additive damage accumulation. However, $\ln(L_W((\theta_1, \theta_2)^\top))$ is the limit of $\ln(L_A((\theta_1, \theta_2, \theta_3)^\top))$ if θ_3 goes to zero. Hence, we have the following corollary.

Corollary II.2: The likelihood function L_W of the load-sharing model without damage accumulation satisfies

$$\begin{aligned}
&\ln(L_W((\theta_1, \theta_2)^\top)) = \ln(L_M((\theta_1, \theta_2, 0)^\top)) \\
&= \lim_{\theta_3 \to 0} \ln(L_A((\theta_1, \theta_2, \theta_3)^\top)) \\
&= \sum_{j=1}^{J} \left\{ \sum_{i=1}^{I_j} [-\theta_1 + \theta_2 \ln(a_{ij}) - \ln(\tau)] \right. \\
&\quad \left. - \frac{\exp(-\theta_1)}{\tau} \left[\sum_{i=1}^{I_j+1} a_{ij}^{\theta_2} W_{ij} \right] \right\}.
\end{aligned} \tag{10}$$

Note that the likelihood function in (10) would also be obtained if one uses the fact that the waiting times W_{ij} in the pure load-sharing system are independent with exponential distribution with parameter $\frac{1}{\tau} \exp(-\theta_1) a_{ij}^{\theta_2}$.

C. Simulating the Processes

For calculating the proposed prediction intervals and for conducting a simulation study, the damage accumulation point processes must be simulated.

Observations from the load-sharing model without damage accumulation can be easily simulated since the interarrival times W_{ij} have exponential distributions with parameters $\frac{1}{\tau} \exp(-\theta_1) a_{ij}^{\theta_2}$. The simulation of a load-sharing model with damage accumulation is more complicated. We adopt here a method which is used for the generation of a nonhomogeneous Poisson process; see, e.g., [39]. Therefore, note that the intensity function λ_j can be interpreted as a conditional hazard rate given

by [36]

$$\lambda_j(t) = h_{ij}(t|t_{1,j},\ldots,t_{i-1,j}) := \frac{f_{i,j}(t|t_{1,j},\ldots,t_{i-1,j})}{S_{ij}(t|t_{1,j},\ldots,t_{i-1,j})}$$

for $t_{i-1,j} < t \leq t_{i,j}$ where $f_{i,j}(t|t_{1,j},\ldots,t_{i-1,j})$ is the conditional density of $T_{i,j}$ given $T_{1,j} = t_{1,j},\ldots,T_{i-1,j} = t_{i-1,j}$ and

$$S_{ij}(t|t_{1,j},\ldots,t_{i-1,j}) := 1 - \int_{t_{i-1,j}}^{t} f_{ij}(u|t_{1,j},\ldots,t_{i-1,j})du$$

is the associated survival function with $S_{ij}(t_{i-1,j}|t_{1,j},\ldots,t_{i-1,j}) = 1$. Let

$$H_{ij}(t|t_{1,j},\ldots,t_{i-1,j}) := \int_{t_{i-1,j}}^{t} h_{ij}(u|t_{1,j},\ldots,t_{i-1,j})du = \int_{t_{i-1,j}}^{t} \lambda_j(u)du$$

be the cumulative conditional hazard function.

Lemma II.3: The conditional distribution of $H_{ij}(T_{i,j}|T_{1,j},\ldots,T_{i-1,j})$ given $T_{1,j} = t_{1,j},\ldots,T_{i-1,j} = t_{i-1,j}$ is an exponential distribution with parameter 1.

To simulate the random variables $T_{i,j}$ for $i = 1,\ldots,I_j$, $j = 1,\ldots,J$, one can now simulate independent random variables $Y_{i,j}$ with exponential distribution with parameter 1 for $i = 1,\ldots,I_j$, $j = 1,\ldots,J$ and then apply the inverse cumulative conditional hazard function on these variables. Hence, set the cumulative conditional hazard functions of the Models *M*, *A*, and *W*, respectively, to

$$\Lambda_{ij}^{M}(t) := H_{ij}^{M}(t|t_{1,j},\ldots,t_{i-1,j}) := \int_{t_{i-1,j}}^{t} \lambda_j^{M}(u)du,$$

$$\Lambda_{ij}^{A}(t) := H_{ij}^{A}(t|t_{1,j},\ldots,t_{i-1,j}) := \int_{t_{i-1,j}}^{t} \lambda_j^{A}(u)du,$$

$$\Lambda_{ij}^{W}(t) := H_{ij}^{W}(t|t_{1,j},\ldots,t_{i-1,j}) := \int_{t_{i-1,j}}^{t} \lambda_j^{W}(u)du$$

where $t_{i-1,j} < t \leq t_{i,j}$. Then $(\Lambda_{ij}^{M})^{-1}(Y_{i,j})$, $(\Lambda_{ij}^{A})^{-1}(Y_{i,j})$, and $(\Lambda_{ij}^{W})^{-1}(Y_{i,j})$ have the same distributions as the observations $T_{i,j}^{M}$, $T_{i,j}^{A}$, and $T_{i,j}^{W}$ of the Models *M*, *A*, and *W*, respectively. This holds for $i = 1,\ldots,I_j$, $j = 1,\ldots,J$.

Theorem II.4: The cumulative conditional hazard functions of the load-sharing models with multiplicative damage accumulation and with additive damage accumulation and their inverses are given by

$$\Lambda_{ij}^{M}(t) = \frac{\exp(-\theta_1)\, a_{ij}^{\theta_2-1}}{\tau^{\theta_3+1}\,(\theta_3+1)} \left[(a_{ij}t - a_{ij}t_{i-1,j} + C_j(i-1))^{\theta_3+1} - C_j(i-1)^{\theta_3+1}\right],$$

$$(\Lambda_{ij}^{M})^{-1}(y) = \frac{1}{a_{ij}} \left[\left(\frac{\tau^{\theta_3+1}\,(\theta_3+1)}{\exp(-\theta_1)\, a_{ij}^{\theta_2-1}} y + C_j(i-1)^{\theta_3+1}\right)^{\frac{1}{\theta_3+1}} + a_{ij}t_{i-1,j} - C_j(i-1)\right],$$

$$\Lambda_{ij}^{A}(t) = \frac{\exp(-\theta_1)}{\theta_3(\theta_2+1)a_{ij}} \left[\left(\frac{\theta_3 a_{ij}}{\tau}t + a_{ij} - \frac{\theta_3}{\tau}\left[a_{ij}t_{i-1,j} - C_j(i-1)\right]\right)^{\theta_2+1} - \left(a_{ij} + \theta_3\frac{1}{\tau}\,C_j(i-1)\right)^{\theta_2+1}\right],$$

$$(\Lambda_{ij}^{A})^{-1}(y) = \frac{\tau}{\theta_3 a_{ij}} \left[\left(\frac{\theta_3(\theta_2+1)a_{ij}}{\exp(-\theta_1)} y + \left(a_{ij} + \theta_3\frac{1}{\tau}\,C_j(i-1)\right)^{\theta_2+1}\right)^{\frac{1}{\theta_2+1}} - a_{ij} + \frac{\theta_3}{\tau}\left[a_{ij}t_{i-1,j} - C_j(i-1)\right]\right].$$

Note that we obtain $(\Lambda_{ij}^{M})^{-1}(0) = t_{i-1,j}$ and $(\Lambda_{ij}^{A})^{-1}(0) = t_{i-1,j}$ for both models. Moreover, it holds for $\theta_3 = 0$

$$\Lambda_{ij}^{M}(t) = \frac{\exp(-\theta_1)}{\tau}\, a_{ij}^{\theta_2}(t - t_{i-1,j}) = \Lambda_{ij}^{W}(t)$$

and

$$(\Lambda_{ij}^{M})^{-1}(y) = \frac{\tau}{\exp(-\theta_1)\, a_{ij}^{\theta_2}} y + t_{i-1,j} = (\Lambda_{ij}^{W})^{-1}(y)$$

so that $(\Lambda_{ij}^{M})^{-1}(Y_{ij}) - t_{i-1,j} = \frac{\tau}{\exp(-\theta_1)\, a_{ij}^{\theta_2}} Y_{ij}$ has an exponential distribution with parameter $\frac{\exp(-\theta_1)}{\tau}\, a_{ij}^{\theta_2}$ if Y_{ij} has an exponential distribution with parameter 1. For the load-sharing model with additive damage accumulation, we get

$$\lim_{\theta_3 \to 0} \Lambda_{ij}^{A}(t) = \frac{\exp(-\theta_1)}{\tau}\, a_{ij}^{\theta_2}(t - t_{i-1,j}) = \Lambda_{ij}^{W}(t) \qquad (11)$$

and

$$\lim_{\theta_3 \to 0} (\Lambda_{ij}^{A})^{-1}(y) = \frac{\tau}{\exp(-\theta_1)\, a_{ij}^{\theta_2}} y + t_{i-1,j} = (\Lambda_{ij}^{W})^{-1}(y). \qquad (12)$$

The proofs of (11) and (12) are similar to that of Corollary II.2 concerning the model with additive damage accumulation.

III. Statistical Methods

In this section, both a frequentist and a Bayesian approach to parameter estimation, model comparison, and prediction of the load-sharing models with and without damage accumulation will be detailed. Both approaches make use of the likelihood functions given in Section II-B.

A. Frequentist Estimators, Tests, and Prediction Intervals

For calculating the ML estimators, note that both log-likelihood functions for the load-sharing models with damage

accumulation given by (8) and (9) can be written as

$$\ln(L(\theta)) = -\theta_1 \sum_{j=1}^{J} I_j + B_1(\theta_2,\theta_3) - \exp(-\theta_1) B_2(\theta_2,\theta_3)$$

where B_1 and B_2 are functions of θ_2 and θ_3 which do not depend on θ_1. For the load-sharing models without damage accumulation, we also get this form by dropping θ_3 so that B_1 and B_2 depend only on θ_2. Hence, for the load-sharing models with damage accumulation, we have

$$\begin{aligned}\frac{\partial}{\partial\theta_1}\ln(L(\theta)) = -\sum_{j=1}^{J} I_j + \exp(-\theta_1) B_2(\theta_2,\theta_3) = 0 \\ \iff \exp(-\theta_1) = \frac{\sum_{j=1}^{J} I_j}{B_2(\theta_2,\theta_3)} \\ \iff \theta_1 = \widehat{\theta}_1(\theta_2,\theta_3) := -\ln\left(\frac{\sum_{j=1}^{J} I_j}{B_2(\theta_2,\theta_3)}\right).\end{aligned}$$

Thus, the log-likelihood

$$\begin{aligned}&\ln(L((\widehat{\theta}_1(\theta_2,\theta_3),\theta_2,\theta_3))) \\ &= \ln\left(\frac{\sum_{j=1}^{J} I_j}{B_2(\theta_2,\theta_3)}\right)\sum_{j=1}^{J} I_j + B_1(\theta_2,\theta_3) - \sum_{j=1}^{J} I_j\end{aligned}$$

becomes effectively a function of just two parameters, facilitating its maximization. For the load-sharing models without damage accumulation, the optimization is even simpler since then only a function of one parameter needs to be maximized. The optimization can be implemented with the `R` function `optim` of [40].

The hypothesis $H_0 : \theta_3 = 0$ of no damage accumulation can be tested by a likelihood ratio test using the log-likelihood functions evaluated at the ML estimates. Let $L_{\mathcal{M}} = L_M$ or $L_{\mathcal{M}} = L_A$, respectively, be the likelihood function for the load-sharing model with multiplicative or additive damage accumulation and $\widehat{\theta}_{\mathcal{M}} \in \mathbb{R}^3$ the corresponding ML estimate, let L_W be the likelihood function for the load-sharing model without damage accumulation and $\widehat{\theta}_W \in \mathbb{R}^2$ the corresponding ML estimate, and let $\chi^2_{1,1-\alpha}$ be the $(1-\alpha)$-quantile of the χ^2-distribution with one degree of freedom. Then an asymptotic α-level test for $H_0 : \theta_3 = 0$ in model $\mathcal{M}$ is given by

reject $H_0 : \theta_3 = 0$ if

$$-2\left(\ln(L_W(\widehat{\theta}_W)) - \ln(L_{\mathcal{M}}(\widehat{\theta}_{\mathcal{M}}))\right) > \chi^2_{1,1-\alpha}. \qquad (13)$$

Similarly, to test the hypothesis $H_0 : \theta = \theta_*$ for a given parameter vector θ_*, also a likelihood ratio test using the log-likelihood functions at the ML estimates can be used. For this test, let $L_{\mathcal{M}} = L_M$, $L_{\mathcal{M}} = L_A$, or $L_{\mathcal{M}} = L_W$, respectively, be the likelihood function for the load-sharing model with multiplicative or additive damage accumulation or without damage accumulation and $\widehat{\theta}_{\mathcal{M}}$ the corresponding ML estimate, and let $\chi^2_{r,1-\alpha}$ be the $(1-\alpha)$-quantile of the χ^2-distribution with r degree of freedom where $r = 3$ for the models with damage accumulation and $r = 2$ for the model without damage accumulation is used. Then an asymptotic α-level test for $H_0 : \theta = \theta_*$ in model $\mathcal{M}$ is given by

reject $H_0 : \theta = \theta_*$ if

$$-2\left(\ln(L_{\mathcal{M}}(\theta_*)) - \ln(L_{\mathcal{M}}(\widehat{\theta}_{\mathcal{M}}))\right) > \chi^2_{r,1-\alpha}. \qquad (14)$$

To obtain the asymptotic distributions of both tests, it is necessary to assume that the different processes $\mathcal{N}_j(t)_{t\le\tau_j}$, $j = 1,\ldots,J$, are independent and that J converges to ∞. Moreover, some assumptions on the stress levels $s_1,\ldots,s_J$ and the time horizons $\tau_1,\ldots,\tau_J$ are needed; see, e.g., [41] and [42, pp. 458]. A simple assumption is that $(s_1,\tau_1),\ldots,(s_J,\tau_J)$ are realizations of independent and identically distributed (i.i.d.) variables $(S_1,\mathcal{T}_1),\ldots,(S_J,\mathcal{T}_J)$ so that the processes are i.i.d. Moreover, the distribution of $(S_j,\mathcal{T}_j)$ should ensure that enough failures in a process can be observed. In particular, S_j and $\mathcal{T}_j$ should be negatively correlated. Nevertheless, the question is whether these tests keep the level α for finite samples. This will be answered by the simulation study in Section V.

Hereinafter, $\mathcal{M} = M, A, W$ denotes the model with multiplicative, additive, and without damage accumulation, respectively. By the duality between tests and confidence sets, an asymptotic frequentist $(1-\alpha)$-confidence set $\mathbb{C}^F_{\mathcal{M},1-\alpha}$ for θ is given by

$$\begin{aligned}&\mathbb{C}^F_{\mathcal{M},1-\alpha} \\ &:= \left\{\theta;\ -2\left(\ln(L_{\mathcal{M}}(\theta)) - \ln(L_{\mathcal{M}}(\widehat{\theta}_{\mathcal{M}}))\right) \le \chi^2_{r,1-\alpha}\right\}.\end{aligned}$$

The confidence sets can be calculated by grid search; see Section IV-C.

If a new point process $N_0(t)_{t\le\tau_0}$ with initial stress s_0 is observed until τ_0 with I_0 failures, then all available observations for predicting the time $T_{I_c,0}$ of a future I_cth failure in the new process with $I_c > I_0$ is given by $\mathbf{N}_0 := \{N_j(t)_{t\le\tau_j};\ j = 0,1,\ldots,J\}$ which is a realization of $\boldsymbol{\mathcal{N}}_0 := \{\mathcal{N}_j(t)_{t\le\tau_j};\ j = 0,1,\ldots,J\}$. If $q^{\mathcal{M}}_\alpha(\theta)$ is the α-quantile of the predictive distribution of the I_cth failure time $T_{I_c,0}$, given $N_0(t)_{t\le\tau_0}$ in model $\mathcal{M}$, then an asymptotic $(1-\alpha)$-prediction interval $\mathbb{P}^F_{\mathcal{M},1-\alpha}(\mathbf{N}_0)$ for the future failure time $T_{I_c,0}$ is given by

$$\mathbb{P}^F_{\mathcal{M},1-\alpha}(\mathbf{N}_0) := \bigcup_{\theta\in\mathbb{C}^F_{\mathcal{M},1-\alpha/2}} \left[q^{\mathcal{M}}_{\alpha/4}(\theta), q^{\mathcal{M}}_{1-\alpha/4}(\theta)\right]. \qquad (15)$$

To facilitate the calculation of $P^F_{\mathcal{M},1-\alpha}(\mathbf{N}_0)$, one can use a slightly larger prediction interval by calculating

$$\left[\min_{\theta\in\mathbb{C}^F_{\mathcal{M},1-\alpha/2}} q^{\mathcal{M}}_{\alpha/4}(\theta), \max_{\theta\in\mathbb{C}^F_{\mathcal{M},1-\alpha/2}} q^{\mathcal{M}}_{1-\alpha/4}(\theta)\right].$$

Note that $\mathbb{C}^F_{\mathcal{M},1-\alpha/2}$ may depend on $\mathbf{N}_0$ or $\mathbf{N} := \{N_j(t)_{t\le\tau_j};\ j = 1,\ldots,J\}$.

Lemma III.1: The prediction interval given by (15) satisfies

$$\lim_{J\to\infty} \Pr_\theta(T_{I_c,0} \in \mathbb{P}^F_{\mathcal{M},1-\alpha}(\boldsymbol{\mathcal{N}}_0)) \ge 1-\alpha$$

for all θ of model $\mathcal{M}$.

In the model without damage accumulation, the predictive distribution is the hypoexponential distribution so that the quantiles $q_\alpha^W(\theta)$ can be calculated from this distribution as in [19]. However, for the models with damage accumulation, the quantiles can be determined only by simulating the process N_0 starting at τ_0. For simulating N_0 with $\mathcal{M} = M, A$, see Section II-C.

B. Bayesian Estimators and Prediction Intervals

The Bayesian approach to statistical inference treats the parameters $\theta = (\theta_1, \theta_2, \theta_3)$ as unknown random variables with a joint prior probability distribution. Inference is based on their posterior distribution, given the observed point processes $\mathbf{N} = \{N_j(t)_{t\leq\tau_j}; j = 1, \ldots, J\}$. According to Bayes' theorem, the joint posterior distribution is proportional to prior $\times$ likelihood, i.e.,

$$p(\theta|\mathbf{N}) \propto p(\theta)L(\mathbf{N}|\theta)$$

with $L(\mathbf{N}|\theta) = L_W(\theta), L_M(\theta)$, or $L_A(\theta)$, respectively, as defined in Section II-B. The Bayesian approach allows prior information to be taken into account by eliciting informative prior distributions. However, here, we use noninformative location- and scale-invariant priors, respectively, i.e., $p(\theta_1) \propto 1$ and $p(\theta_i) \propto \frac{1}{\theta_i}$ for $i = 2, 3$.

As the posterior distribution is fairly complex, it precludes an analytic marginalization in closed form. Posterior computation is, therefore, based on Markov chain Monte Carlo (MCMC) simulations. More specifically, Gibbs sampling is employed using the implementation in the Bayesian software package JAGS; see [43]. We have already calculated the log-likelihood functions for each model in Section II-B. In order to specify a likelihood in JAGS that is not included in its list of standard distributions, we make use of the so-called "zeros trick" described in [44]. Each of the J systems contributes a likelihood term $L[j]$ given by the sum in curly brackets in (8), (9), and (10) to L_M, L_A, and L_W, respectively. If we specify J independent pseudo-observations all with the value of 0 and assign these a Poisson distribution with mean $\mu_j = -\ln(L[j]) + c$, the correct likelihood function will be constructed in JAGS. An arbitrary constant c can be added to μ_j to ensure that the means are positive. Any multiplicative constant in the likelihood function will not affect the posterior distribution because it cancels when applying Bayes' theorem as it is included in both numerator and denominator.

To compare the relative fit of the three Bayesian models, we use the deviance information criterion (DIC) [45] which combines a measure of goodness-of-fit and a measure of complexity, both based on the deviance. The goodness-of-fit measure is the posterior mean of the deviance $D(\theta) = -2\log L(\mathbf{N}|\theta)$. The number of independent parameters is often not well-defined in Bayesian models when using informative priors and hierarchical structures because the prior restricts the parameter space. As an estimate of the so-called effective number of parameters, the difference of the posterior mean of the deviance and the deviance evaluated at the posterior mean was suggested, i.e., $p_D = \bar{D}(\theta) - D(\bar{\theta})$. The DIC is then defined as

$$\text{DIC} = \bar{D}(\theta) + p_D$$

and thus trades off the fit of a model against its effective number of parameters.

In Bayes analysis, prediction is based on the posterior predictive distribution. However, the posterior predictive distribution is complicated for load-sharing models with damage accumulation. Therefore, prediction intervals here are obtained similarly to the frequentist approach in (15) by using

$$\mathbb{P}^B_{\mathcal{M},1-\alpha}(\mathbf{N}_0) := \bigcup_{\theta\in\mathbb{C}^B_{\mathcal{M},1-\alpha/2}} \left[q^{\mathcal{M}}_{\alpha/4}(\theta), q^{\mathcal{M}}_{1-\alpha/4}(\theta)\right] \qquad (16)$$

where only the confidence set $\mathbb{C}^F_{\mathcal{M},1-\alpha/2}$ is replaced by the credible set $\mathbb{C}^B_{\mathcal{M},1-\alpha/2}$ and $\mathcal{M} = M, A, W$ again denotes the model with multiplicative, additive, and without damage accumulation, respectively. The $(1-\alpha)$-credible set $\mathbb{C}^B_{\mathcal{M},1-\alpha}$ is a set which has a posterior probability of $1-\alpha$. As in the frequentist case, it may only depend on the past processes given by $\mathbf{N}$ or on all available observations up to τ_0 given by $\mathbf{N}_0$.

Lemma III.2: The prediction interval for model $\mathcal{M}$ given by (16) satisfies

$$\begin{aligned}&\Pr(T_{I_c,0} \in \mathbb{P}^B_{\mathcal{M},1-\alpha}(\boldsymbol{\mathcal{N}}_0))\\ &= \int \Pr(T_{I_c,0} \in \mathbb{P}^B_{\mathcal{M},1-\alpha}(\boldsymbol{\mathcal{N}}_0)|\theta)\; p(\theta)\; d(\theta) \geq 1-\alpha.\end{aligned}$$

The $(1-\alpha)$-credible set $\mathbb{C}^B_{\mathcal{M},1-\alpha}$ can be obtained by a proportion of $1-\alpha$ of all parameters of the Markov chain after the burn-in phase and after thinning. To obtain a narrow set that contains a proportion of $1-\alpha$ of these posterior parameters, we use the half space depth of Tukey [46]. Tukey's half space depth provides a ranking of multidimensional data points from the most central data points to least central points. The centrality of a data point is given by the minimum relative number of data points which must be removed so that there is a half space containing only the considered data point. An extremal point of the data cloud has the smallest depth since a half space exists which includes only this extremal point. The highest depths are obtained by data points in the center of the data cloud. Here, we calculate the half space depth via the R package `ddalpha` of [47] and determine the smallest set with a proportion of $1-\alpha$ by the empirical α-quantile of the depth values.

IV. Application to Data From Experiments With Concrete Beams

In this lab experiment, $J = 10$ prestressed concrete beams were exposed to cyclic loads where time is measured in number of load cycles. The cyclic load means that an external stress varies between a minimum stress $s_{\min}$ and a maximum stress $s_{\max}$ so that the stress range $s_{\max} - s_{\min}$ is the initial stress s_j here. Each beam consisted of $\mathcal{K}_j = 35$ tension wires which broke successively. Because each break of a tension wire provides a loud noise, the exact time points where each of the single tension wires broke were determined with a microphone. For the ten experiments, Table I provides the different stress levels given by the initial stress ranges s_j, the number of observed breaks I_j, and the number of load cycles until the last observed failure $t_{I_j,j}$ and the end of the experiment τ_j, while Fig. 1 shows all time points

TABLE I
EXPERIMENTS WITH THE STRESS LEVELS s_j GIVEN BY STRESS RANGES, THE OBSERVED NUMBER OF BREAKS, LOAD CYCLES UNTIL LAST FAILURE, AND THE LAST TIME POINTS OF THE EXPERIMENTS

beam	stress range s_j in MPa	number I_j of observed breaks	time $t_{I_j,j}$ in number of load cycles until last observed break (in millions)	end τ_j of the experiment (in millions)
TR01	200	15	3.388	3.388
TR02	455	9	0.206	0.206
TR03	200	12	3.474	3.474
TR04	150	7	5.465	5.521
TR05	98	4	15.070	15.390
SB01	200	17	5.657	5.657
SB02	100	18	16.193	16.193
SB03	60	18	85.157	85.157
SB04	80	20	21.625	22.122
SB05	80	19	66.472	66.472

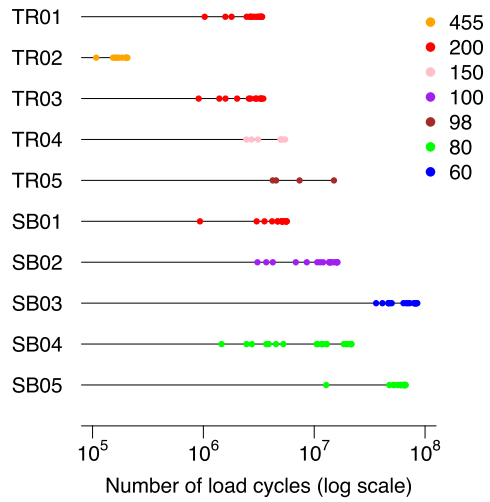

Fig. 1. Time points of successive fractures of tension wires.

of successive fractures of tension wires for all experiments. In most cases, the end point of the experiment coincides with the time point of the last observed break since this is the critical one where the whole beam failed. The experiments denoted by TR and SB differ in the frequency of load cycles. In the experiments denoted by SB, the frequency of load cycles was increased so that up to 108 000 million load cycles could be observed and thereby also failures of tension wires at low stress levels.

We assume here that each tension wire carries the same load so that an equal load-sharing system where $a_j(t)$ is given by (2) is appropriate. The authors in [19] showed that the equal load-sharing model without damage accumulation fits the data quite well. This was shown by a Q-Q plot with a confidence band, a leave-one-out analysis, and by a prediction interval for a stress level lower than the observed stress levels that indeed included the future observation. However, the question remained whether there is really no damage accumulation between the breaks. Now, the answer to this question can be given.

TABLE II
SCALE-INVARIANT ML ESTIMATES AND CORRESPONDING 95% CONFIDENCE INTERVALS FOR THE LOAD-SHARING MODELS WITHOUT DAMAGE ACCUMULATION (*W*), WITH MULTIPLICATIVE DAMAGE ACCUMULATION (*M*), AND WITH ADDITIVE DAMAGE ACCUMULATION (*A*)

Model	θ_1	θ_2	θ_3
W			
estimate	0.827	2.902	
confidence interval	(0.203, 1.488)	(2.500, 3.301)	
M			
estimate	1.698	3.450	0.397
confidence interval	(0.777, 2.699)	(2.875, 4.034)	(0.160, 0.656)
A			
estimate	2.039	3.462	0.186
confidence interval	(0.869, 3.301)	(2.842, 4.084)	(0.052, 0.319)

TABLE III
LOG-LIKELIHOOD FUNCTIONS FOR THE SCALE-INVARIANT ML ESTIMATES OF TABLE II IN THE LOAD-SHARING MODELS WITHOUT DAMAGE ACCUMULATION (*W*), WITH MULTIPLICATIVE DAMAGE ACCUMULATION (*M*), AND WITH ADDITIVE DAMAGE ACCUMULATION (*A*), WHERE fac DENOTES THE FACTOR BY WHICH THE TIME VARIABLE IS DIVIDED

	Loglikelihood for fac		
Model	1	10^3	10^6
W	-1994.15	-1033.98	-73.80
M	-1983.05	-1022.88	-62.70
A	-1986.90	-1026.72	-66.54

TABLE IV
SCALE-DEPENDENT ML ESTIMATES WITH FIXED $\tau_\star$ FOR THE LOAD-SHARING MODELS WITH MULTIPLICATIVE DAMAGE ACCUMULATION (*M*), WITH ADDITIVE DAMAGE ACCUMULATION (*A*), AND THE CORRESPONDING LOG-LIKELIHOOD FUNCTIONS, WHERE fac DENOTES THE FACTOR BY WHICH THE TIME VARIABLE IS DIVIDED

		Model M		Model A	
	fac	$\tau_\star = 10^6$	$\tau_\star = 10^3$	$\tau_\star = 10^6$	$\tau_\star = 10^3$
θ_1	1	6.038	15.686	5.148	7.383
θ_1	10^3	-3.670	6.038	-1.762	5.148
θ_1	10^6	-13.258	-3.670	-8.669	-1.762
θ_2	1	3.450	3.450	3.463	0.000
θ_2	10^3	3.450	3.450	3.462	3.463
θ_2	10^6	3.450	3.450	3.462	3.462
θ_3	1	0.397	0.397	0.00833	2.3562
θ_3	10^3	0.397	0.397	8.314	0.00833
θ_3	10^6	0.397	0.397	8314.378	8.314
Lik	1	-1983.05	-1983.05	-1986.90	-2125.42
Lik	10^3	-1022.88	-1022.88	-1026.72	-1026.72
Lik	10^6	-62.70	-62.70	-66.54	-66.54

A. *Frequentist Estimators and Tests*

Tables II, III, and IV provide the ML estimates, 95% confidence intervals, and the log-likelihoods for the load-sharing models without and with multiplicative and with additive damage accumulation. Numerical optimization was implemented using the `R` function `optim` with the method `L-BFGS-B`. Starting values were set to $(\theta_2, \theta_3)^\top = (3, 2)^\top$ for the models with damage accumulation and $\theta_2 = 3$ for the models without damage accumulation. Almost the same results were obtained with different choices of starting values. The search area was $[0, 10^5] \times [0, 10^5]$ for the model with multiplicative damage accumulation, $[0, 10^5] \times [10^{-5}, 10^5]$ for the model with additive damage accumulation, and $[0, 10^5]$ for the model without damage accumulation.

TABLE V
P-VALUES OF THE LIKELIHOOD RATIO TESTS GIVEN BY (13) BASED ON THE SCALE-DEPENDENT ML ESTIMATORS AND THE SCALE-INVARIANT ML ESTIMATORS USING $fac = 1$

	scale dependent ML		scale invariant ML
Model	$\tau_\star = 10^3$	$\tau_\star = 10^6$	
M	2.46e-06	2.46e-06	2.46e-06
A	1	1.39e-04	1.39e-04

Tables II and III show ML estimates and log-likelihood values for the scale-invariant case where τ is the mean time horizon $\frac{1}{J}\sum_{j=1}^{J}\tau_j$, while Table IV provides the corresponding results for the scale-dependent versions where τ is the manually given value $\tau_\star$. To study the influence of time scaling, the number of load cycles is divided by factors $fac = 1$, 10^3, and 10^6. For all of these three time scales, the results of Table II remain the same. This is in contrast to Table IV. Here, the parameter θ_1 is influenced by the time scale in all three models. Additionally, the parameter θ_3 of the model with additive damage accumulation changes with different scale factors. However, all estimates are the same when the time and $\tau_\star$ are changed concordantly, i.e., the estimates are the same for $fac = 1$, $\tau_\star = 10^6$ and $fac = 10^3$, $\tau_\star = 10^3$, as well as for $fac = 10^3$, $\tau_\star = 10^6$, and $fac = 10^6$, $\tau_\star = 10^3$. Moreover, the strange results in the last column of Table IV for $fac = 1$ demonstrate that the model with additive damage accumulation has a severe problem if the scale adjustment parameter $\tau_\star$ is chosen too small which is the case here for $\tau_\star = 10^3$ and $fac = 1$.

Tables III and IV show that the model with multiplicative damage accumulation always has the largest likelihood values followed by the model with additive damage accumulation and then the model without damage accumulation. The effect of θ_3 for damage accumulation is indeed significant according to the *p*-values given in Table V. However, Table V also demonstrates that a too small scale adjustment parameter $\tau_\star$ can lead to completely opposite results.

Nevertheless, we can conclude here that damage accumulation has a significant influence on the data from the experiments with concrete beams. This is the case although the likelihood ratio test in its present implementation is too conservative which is shown by the simulation study in Section V.

B. Bayesian Estimation

Samples from the posterior distribution of the parameters of the three models without and with multiplicative and with additive damage accumulation in the scale-invariant version were obtained using JAGS and the R-package `rjags`. We used a burn-in period of 10 000 iterations and ran the Gibbs sampler for a further 40 000 iterations from two different starting values. Convergence of the Markov chain was checked using the R-package `coda`. All chains for the model without and with multiplicative damage accumulation passed the convergence tests. The posterior distribution of the model with additive damage accumulation, however, has many local maxima and the MCMC chains often get stuck in local maxima, depending on the starting value. For posterior inference in the model with additive damage accumulation, we discard the samples of the chain that got stuck in a local maxima and use only the samples of the chain that converged to the global maximum where the ML estimates were used as starting values. Note that discarding some samples may lead to a small bias of the estimates. These convergence problems are most likely due to the large posterior correlations between the parameters. A reparametrization might yield faster mixing chains.

TABLE VI
POSTERIOR MEAN, POSTERIOR STANDARD DEVIATION, AND 95% CENTRAL POSTERIOR CREDIBLE INTERVALS IN THE SCALE-INVARIANT VERSION FOR THE LOAD-SHARING MODELS WITHOUT (*W*) AND WITH MULTIPLICATIVE (*M*) AND WITH ADDITIVE (*A*) DAMAGE ACCUMULATION

Model	θ_1	θ_2	θ_3
W			
mean	0.818	2.889	
standard deviation	0.261	0.163	
credible interval	(0.313, 1.343)	(2.567, 3.210)	
M			
mean	1.646	3.409	0.374
standard deviation	0.347	0.212	0.093
credible interval	(0.980, 2.323)	(2.997, 3.812)	(0.194, 0.558)
A			
mean	1.899	3.389	0.166
standard deviation	0.448	0.229	0.054
credible interval	(1.012, 2.766)	(2.934, 3.828)	(0.048, 0.266)

TABLE VII
POSTERIOR MEAN OF THE DEVIANCE, THE EFFECTIVE NUMBER OF PARAMETERS, AND THE DIC FOR LOAD-SHARING MODELS

Model	$\bar{D}(\theta)$	p_D	DIC
W	3990	0.0117	3990
M	3969	0.034	3969
A	3977	0.035	3977

Table VI gives estimates of the posterior mean and standard deviation of the marginal posterior distributions for each model parameter as well as 95% central posterior credible intervals. These are comparable to the ML estimates of the corresponding models as we are using noninformative prior distributions. Traceplots and kernel density estimates of the marginal posterior distributions of each parameter for each of the three models are given in the supplementary material.

Table VII gives the values of the deviance, the effective number of parameters, and the DIC value for each of the three load-sharing models. The smaller the DIC, the better the model fit. As we do not have a hierarchical structure and use independent priors for the parameters, a penalty term similar to the Akaike information criterion (AIC), i.e., $2\times$ the number of parameters, is also reasonable. The authors in [48] have explored the difficulty of assessing the Monte Carlo error on DIC. As a rule of thumb, a difference of less than 5 is not definitive and a difference of 10 or more in DIC values is deemed a significant difference. Therefore, models with damage accumulation clearly yield a better fit than the model without damage accumulation, confirming the conclusion of the frequentist analysis.

C. Frequentist and Bayesian Prediction Intervals

The authors of [19] provide 90%-prediction intervals for the model without damage accumulation for a new experiment,

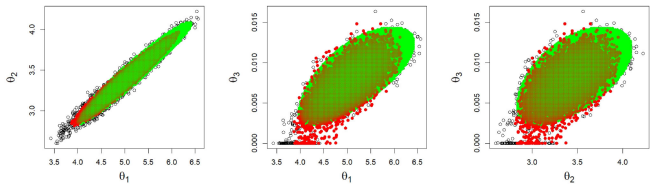

Fig. 2. Two-dimensional projections of the whole set of simulated parameters of the posterior distribution (black), the frequentist 95%-confidence sets (green), and the Bayesian 95%-credible sets (red) for the model with additive damage accumulation in the scale-dependent version with $\tau_\star = 10^6$.

SB06, with an initial stress range of 50 MPa. This stress level is lower than the stress levels of the experiments given in Table I used for estimation and for calculating the prediction intervals. Nevertheless, the calculated prediction interval for the first break included the realized first break. After 108.274 millions of load cycles, i.e., after approximate six months, Experiment SB06 was stopped without showing a second break. The time point of 108.274 millions of load cycles was also included in the prediction interval for the second break. The experiment was restarted as Experiment SB06a with an increased stress range of 120 MPa. Now, the prediction intervals of [19] no longer included the realized time points for the next 17 breaks even though the first tension wire break was taken into account. The explanation provided in [19] was that the first experiment with an initial stress of 50 MPa caused a damage which accumulated up to the 108.274 millions of load cycles where experiment SB06 was stopped.

To calculate the 90%-prediction intervals in the case of the models with multiplicative and additive damage accumulation, 95%-confidence sets were calculated via grids with 101^3 points and 95%-credible sets were calculated via the posterior distribution given by 40 000 (without, multiplicative model) and 8500 (additive model) simulated points. Fig. 2 shows two-dimensional projections of the three-dimensional sets for the model with additive damage accumulation. The projections for the model with multiplicative damage accumulation and the sets for the model without damage accumulation are given in the supplementary material. In particular, only the model with additive damage accumulation provides some problems for the simulated posterior distribution visible by several outliers for θ_3 close to zero as can be seen from Fig. 2. However, the 95%-confidence set and the 95%-credible set are rather similar in the projections on θ_1 and θ_2. This similarity appears in all projections for the model with multiplicative damage accumulation and for the sets for the model without damage accumulation, which once again demonstrates that the model with multiplicative damage accumulation provides more stable results. The only difference between the frequentist confidence sets and the Bayesian credible sets is a small shift of Bayesian credible sets toward zero as visible in the left-hand side of Fig. 2.

For calculating the 90%-prediction intervals, each of the 95%-confidence sets and 95%-credible sets were thinned to approximately 2000 parameters and then the damage accumulation point process was simulated 10 000 times for each of these parameters θ. The quantiles $q^{\mathcal{M}}_{0.025}(\theta)$ and $q^{\mathcal{M}}_{0.975}(\theta)$ of the

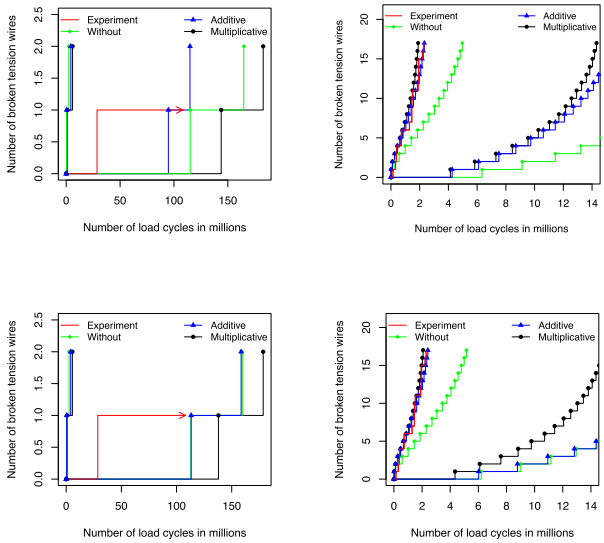

Fig. 3. Frequentist 90%-prediction intervals (first row) and Bayesian 90%-prediction intervals (second row) for the 1st and 2nd breaks for the experiment SB06 exposed to 50 MPa (left-hand side) and the 1st to 17th break for the restarted experiment SB06a exposed to 120 MPa (right-hand side). The red arrow indicates the end of the experiment SB06.

distribution of the I_cth failure time are then approximated by the empirical quantiles of the 10 000 time points of the I_cth event in these 10 000 point processes. To calculate the lower and upper bounds of the prediction interval for the I_cth break, we simply used the minimum of all of the 0.025-quantiles and the maximum of all of the 0.975-quantiles obtained for the parameters θ in the thinned confidence sets and credible sets, respectively. Note that the thinning of the confidence sets and credible sets may shorten the prediction intervals.

The left-hand side of Fig. 3 shows the frequentist and Bayesian prediction intervals for Experiment SB06 based on the three models. All three prediction intervals for the first break include the true time point of the first break. Moreover, the time point of 108.274 millions of load cycles, where Experiment SB06 was stopped, is covered by all prediction intervals for the second break. However, it is very close to the upper bound of the prediction interval for the additive model in the frequentist approach.

The frequentist and Bayesian prediction intervals for the 1st to 17th break of the restarted Experiment SB06a are shown on the right-hand side of Fig. 3. As in [19], the prediction intervals for the model without damage accumulation do not include the failure times of this restarted experiment although the calculation is based on 34 instead of 35 tension wires since one was broken in Experiment SB06. To include the damage caused by Experiment SB06, the damage accumulation of $28\,616\,915 * 50/35 + (108\,273\,608 - 28\,616\,915) * 50/34$ was added to the $C_j(i)$ $(j = 0)$ in (7) since the first break in Experiment SB06 happens at 28 616 915 load cycles. Now the prediction intervals for the model with multiplicative and additive damage accumulation include the failure times of Experiment SB06a. However, this is not always the case. The reason could lie

TABLE VIII
INITIAL (EXTERNAL) STRESS LEVELS s_j, MAXIMAL TEST DURATION τ_j, AND NUMBER $\mathcal{K}_j$ OF COMPONENTS WHICH ARE K TIMES REPEATED IN THE SIMULATION STUDY

		fixed time horizon		fixed number of failures	
s_j	$\mathcal{K}_j$	τ_j	$\tau_\star$	I_j	$\tau_\star$
200	35	2	16	20	16
100	35	16	16	20	16
80	35	30	16	20	16

TABLE IX
PARAMETER VECTOR θ USED IN THE SIMULATION STUDY

Model	θ_1	θ_2	θ_3
W	0.8	2.9	
M	1.7	3.5	0.4
A	2.0	3.5	0.2

in the computation or in the model specification for damage accumulation.

Comparing the frequentist and Bayesian prediction intervals, we see that they are very similar for the models without and with multiplicative damage accumulation. However, the upper bounds for the Bayesian prediction intervals for the model with additive damage accumulation are much larger than that of the frequentist prediction intervals. In particular, these upper bounds are very similar to the upper bounds obtained for the model without damage accumulation. This is caused by the shift of the credible set in the direction of a value of θ_3 close to zero as can be seen in Fig. 2.

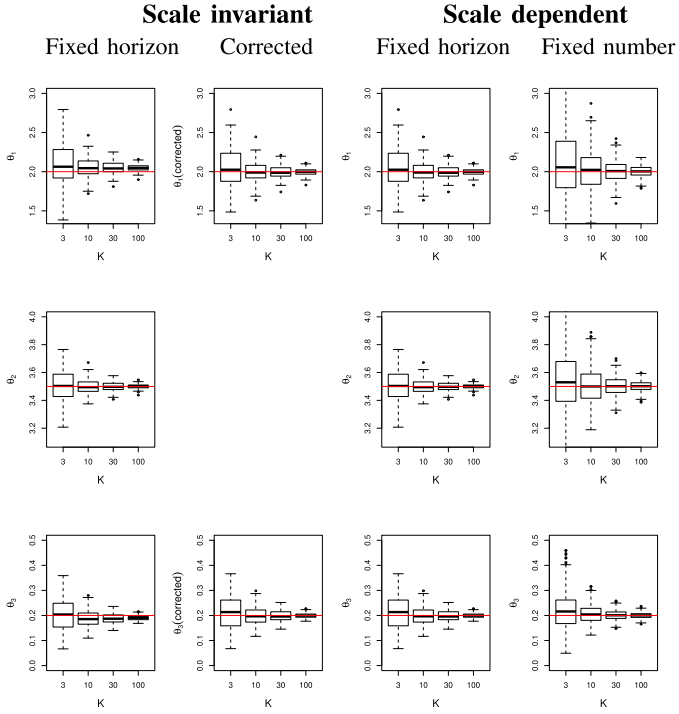

Fig. 4. Boxplots of the estimates for $\theta = (\theta_1, \theta_2, \theta_3)^\top$ for the simulated load-sharing model with additive damage accumulation. First column: scale-invariant estimator in the scenario with fixed horizon. Second column: correction of the scale-invariant estimator. Third column: scale-dependent estimator in the scenario with fixed horizon. Fourth column: scale-dependent estimator in the scenario with fixed number of failures. The red line marks the true parameter.

V. SIMULATION STUDY

A. Setup of the Simulation Study

To mimic the real experiments as closely as possible, we repeatedly (K times) simulated the point processes with the initial stress levels s_j, maximal test duration τ_j, and number $\mathcal{K}_j$ of components given by Table VIII. This means that one experiment had $J = 3\,K$ runs resulting in $J = 3\,K$ point processes. For the scale-dependent estimators, we used $\tau_\star = 16$ for simulating the data as well as for estimation. For the scale-invariant estimators, $\tau_\star = 16$ was also used for the simulating the data, but a data dependent τ was used for estimation.

Additionally, we simulated experiments with a given number I_j of failures instead of the fixed time horizon τ_j. The specification for these simulations can also be seen in Table VIII. In this scenario, only the scale-dependent version with fixed $\tau_\star$ makes sense.

The parameter vector θ was chosen close to the values estimated in the real data set with the scale-invariant estimator and are given by Table IX.

The experiments for the ML estimates were repeated 500 times. Note that already 100 repetitions led to accurate results. However, for the likelihood ratio tests, we used 5000 repetitions.

B. Simulation Results for Estimators

Fig. 4 shows the ML estimators for simulated experiments of the model with additive damage accumulation where each experiment included $J = 3\,K$ simulated point processes and $K = 3, 10, 30, 100$ was used. The first column of these figures shows a bias for the scale-invariant estimators of θ_1 and θ_3. The results for the models with multiplicative damage accumulation and without damage accumulation are similar although the bias appears only for θ_1. The bias is caused by the fact that often the maximal test durations τ_j are not reached because $\mathcal{K}_j = 35$ failures happen before τ_j. This means that the simulated data may consist of τ_j^{Data} which are smaller than the maximal test durations τ_j used for simulating the data via Λ_{ij}^{-1} given by Theorem II.4. However, the estimates can be corrected by using the following properties of the intensity functions:

$$\begin{aligned}
&\lambda_j^M(t) \\
&\quad = \exp(-\theta_1 - \ln(\tau))\, a_j(t)^{\theta_2} \left(\frac{1}{\tau} A_j(t)\right)^{\theta_3} \\
&\quad = \exp(-[\theta_1 + \ln(\tau)(1+\theta_3)])\, a_j(t)^{\theta_2} A_j(t)^{\theta_3} \\
&\quad = \exp\Big(-\Big[\theta_1 + \ln\Big(\frac{\tau}{\tau^{\text{Data}}}\Big)(1+\theta_3) \\
&\qquad + \ln(\tau^{\text{Data}})(1+\theta_3)\Big]\Big)\; a_j(t)^{\theta_2} A_j(t)^{\theta_3}
\end{aligned}$$

for the model with multiplicative damage accumulation and

$$\begin{aligned}
&\lambda_j^A(t) \\
&\quad = \exp(-\theta_1 - \ln(\tau)) \left(a_j(t) + \theta_3 \frac{1}{\tau} A_j(t)\right)^{\theta_2}
\end{aligned}$$

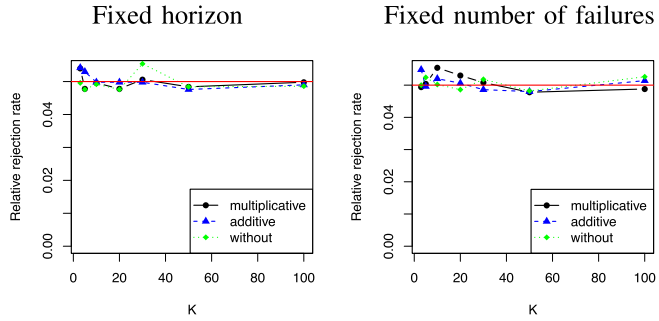

Fig. 5. Rejection rates of the likelihood ratio test for testing the null hypothesis $H_0 : \theta = \theta_*$ in the models with multiplicative damage accumulation, additive damage accumulation, and without damage accumulation. On the left: scenario with fixed horizon. On the right: scenario with fixed number of failures. The red line marks the test level of 0.05.

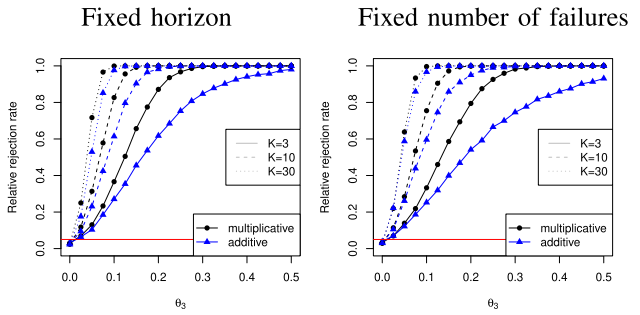

Fig. 6. Rejection rates of the likelihood ratio test at different values of parameter θ_3 for testing the null hypothesis $H_0 : \theta_3 = 0$ in the models with multiplicative damage accumulation and additive damage accumulation. On the left: scenario with fixed horizon. On the right: scenario with fixed number of failures. The red line marks the test level of 0.05.

$$= \exp\left(-\left[\theta_1 + \ln\left(\frac{\tau}{\tau^{\text{Data}}}\right) + \ln(\tau^{\text{Data}})\right]\right) \cdot \left(a_j(t) + \theta_3 \frac{\tau^{\text{Data}}}{\tau} \frac{1}{\tau^{\text{Data}}} A_j(t)\right)^{\theta_2}$$

for the model with additive damage accumulation, where

$$\tau = \frac{1}{J}\sum_j^J \tau_j, \quad \tau^{\text{Data}} = \frac{1}{J}\sum_j^J \tau_j^{\text{Data}}.$$

Since the model with multiplicative damage accumulation coincides with the model without damage accumulation if $\theta_3 = 0$, the following corrections provide unbiased scale-invariant estimators (see the second column of Fig. 4):

$$\widehat{\theta}_1^{\text{Corr}} := \widehat{\theta}_1 - \ln\left(\frac{\tau}{\tau^{\text{Data}}}\right)(1 + \widehat{\theta}_3) \quad \text{for model } M,$$

$$\widehat{\theta}_1^{\text{Corr}} := \widehat{\theta}_1 - \ln\left(\frac{\tau}{\tau^{\text{Data}}}\right) \quad \text{for models } A \text{ and } W,$$

$$\widehat{\theta}_3^{\text{Corr}} := \widehat{\theta}_3 \frac{\tau}{\tau^{\text{Data}}} \quad \text{for model } A.$$

The third column of Fig. 4 provides the results for the scale-dependent estimators. Since the same data were used, these results match those for the corrected scale-invariant estimators. Different results are only obtained in the fourth column where the estimators are applied to the scenario with fixed numbers of failure since the data generation is different. Here, we see a slightly higher variability in all models. This is due to the fact that in the scenario of fixed time horizon, often the maximal number $\mathcal{K}_j = 35$ of possible failures are reached. Hence, more information is available than in the scenario where the maximum number of failures is fixed by $I_j = 20$.

C. Simulation Results for Tests

Fig. 5 provides the rejection rates of the likelihood ratio test for $H_0 : \theta = \theta_*$ given by (14) for the scenarios with fixed time horizon (left column) and fixed number of failures (right column). Here, we obtain exactly the same results for the scale-invariant and the scale-dependent version. With 5000 simulations, the variability of the rejection rates is still high. However, it seems that the tests retain the test level of 0.05 for observation numbers of $J = 3\ K$ with $K = 3, 5, 10, 20, 30, 50, 100$ in all models.

Fig. 6 provides the rejection rates under the null hypothesis and alternatives of the likelihood ratio test given by (13) for testing the null hypothesis of no multiplicative damage accumulation and no additive damage accumulation, respectively, if the data were simulated in the scenario of fixed horizon (left column) and fixed number of failures (right column). Again the results for the scale-invariant and the scale-dependent version are in agreement. Both simulation studies show that both tests are too conservative for observation numbers of $J = 3\ K$ with $K \leq 30$. Nevertheless, the power is quite good. Surprisingly, the power functions are similar although the parameter θ_3 has different meaning in the models with multiplicative and additive damage accumulation.

VI. Conclusion

This article provided the likelihood functions of two models for load-sharing systems with damage accumulation: a model with additive damage accumulation and a model with multiplicative damage accumulation. Both models include the model without damage accumulation as special case so that likelihood ratio tests can be applied to check for a significant damage accumulation effect. The models are given by intensity functions of self-exciting point processes in a scale-invariant and in a scale-dependent version leading to scale-invariant and scale-dependent ML estimators and tests. It was shown that the estimators and tests in the model with additive damage accumulation in the scale-dependent version are very sensitive to the correct scaling of the time scale since the damage accumulation term given by time is added to the load-sharing term which is independent of time. However, the simulation study showed that the scale-invariant estimators have the disadvantage that they must be corrected to obtain unbiased estimators.

For simulating the self-exciting point processes, the cumulative conditional intensity functions and their inverses were calculated explicitly. While the simulation study with 100 repetitions provides sufficient accuracy for the estimators, the variability of the rejection rates of the likelihood ratio tests was still quite high with 5000 simulations. Nevertheless, these simulation results

indicated that the levels of tests for a damage accumulation effect are too conservative in the present implementation. This is potentially due to a problem of finding the global maximum of the likelihood function. We simply used the `R` function `optim` with the method `L-BFGS-B` for optimization. Maybe other optimization methods will improve the power of the tests. Nevertheless, applying these tests to real failures of tension wires of concrete beams leads to significant damage accumulation effects in both models. This holds although Leckey *et al.* [19], who analyzed the same data, came to the conclusion that a load-sharing model without damage accumulation already provides an adequate fit.

In contrast to testing for a damage accumulation effect, the simulations indicated that the test level is retained by testing for a given parameter vector. Hence, these tests can be used to get reasonable small confidence sets for the parameter vectors. These confidence sets were used to obtain prediction intervals for future failures. Applying these prediction intervals to the failures of tension wires of a new concrete beam leads to better results in a restarted experiment than in [19] where a load-sharing model without damage accumulation was considered.

Bayesian parameter estimates and prediction intervals under noninformative priors yielded comparable results to frequentist analysis. Bayesian model selection via DIC confirmed the better fit of the two load-sharing models with damage accumulation compared to the model without damage accumulation. However, as in the frequentist case, the model with additive damage accumulation has more numerical problems. Here, we used the implementation of the Bayesian models in JAGS using the zeros trick.

As an alternative, for the model without damage accumulation, independent exponential waiting times could have been specified and censoring been taken into account as in the approach by [49] for analyzing recurrent event times. This approach also provides a straightforward generalization to more realistic parametric failure time distributions such as the Weibull distribution or even nonparametric failure time distributions within the Bayesian framework. Furthermore, it demonstrates how correlations between subsequent failure times can be taken into account using copulas.

Moreover, other degradation aspects like corrosion may be included in the load-sharing models with damage accumulation as considered for a load-sharing model without damage accumulation in [50]. However, all these avenues are beyond the scope of the current article but could be investigated in future research.

APPENDIX

Proof of Theorem II.1: According to [36, Prop. 7.2.III, p. 232], the likelihood function of realizations $t_1, \ldots, t_{N(\tau)}$ of a point process N on $[0, \tau]$ with left-continuous conditional intensity function $\lambda : [0, T] \to \mathbb{R}$ is given by

$$L = \left[\prod_{i=1}^{N(\tau)} \lambda(t_i) \right] \exp\left(- \int_0^\tau \lambda(t) dt \right). \tag{17}$$

At first, we calculate the term $\int_0^\tau \lambda(t) dt$ for the intensity functions of the two load-sharing models with damage accumulation. For this, note that it holds for $c > 0$ and $v \geq 0$

$$\int_a^b (ct + d)^v dt = \frac{1}{c(v+1)} (ct + d)^{v+1} \Big|_a^b.$$

Set $t_{0,j} = 0$ for $j = 1, \ldots, J$ and recall $N_j(\tau_j) = I_j$.

For the load-sharing model with multiplicative damage accumulation, we get

$$\begin{aligned}
\int_0^{\tau_j} \lambda_j^M(t) dt &= \int_0^{\tau_j} \frac{1}{\tau} \exp(-\theta_1) a_j(t)^{\theta_2} \left(\frac{1}{\tau} A_j(t) \right)^{\theta_3} dt \\
&= \sum_{i=1}^{I_j} \int_{t_{i-1,j}}^{t_{i,j}} \frac{\exp(-\theta_1)}{\tau^{\theta_3+1}} a_{ij}^{\theta_2} A_j(t)^{\theta_3} \, dt \\
&\quad + \int_{t_{I_j,j}}^{\tau_j} \frac{\exp(-\theta_1)}{\tau^{\theta_3+1}} a_{(I_j+1)j}^{\theta_2} A_j(t)^{\theta_3} \, dt \\
&= \frac{\exp(-\theta_1)}{\tau^{\theta_3+1}} \left[\sum_{i=1}^{I_j} a_{ij}^{\theta_2} \int_{t_{i-1,j}}^{t_{i,j}} \left(a_{ij} \left(t - \sum_{k=1}^{i-1} W_{kj} \right) + \sum_{k=1}^{i-1} a_{kj} W_{kj} \right)^{\theta_3} dt \right. \\
&\quad \left. + \, a_{(I_j+1)j}^{\theta_2} \int_{t_{I_j,j}}^{\tau_j} \left(a_{(I_j+1)j} \left(t - \sum_{k=1}^{I_j} W_{kj} \right) + \sum_{k=1}^{I_j} a_{kj} W_{kj} \right)^{\theta_3} dt \right] \\
&= \frac{\exp(-\theta_1)}{\tau^{\theta_3+1}} \left[\sum_{i=1}^{I_j} a_{ij}^{\theta_2} \frac{1}{a_{ij}(\theta_3+1)} \left(a_{ij} \left(t - \sum_{k=1}^{i-1} W_{kj} \right) + \sum_{k=1}^{i-1} a_{kj} W_{kj} \right)^{\theta_3+1} \Bigg|_{t_{i-1,j}}^{t_{i,j}} \right. \\
&\quad \left. + \, a_{(I_j+1)j}^{\theta_2} \frac{1}{a_{(I_j+1)j}(\theta_3+1)} \left(a_{(I_j+1)j} \left(t - \sum_{k=1}^{I_j} W_{kj} \right) + \sum_{k=1}^{I_j} a_{kj} W_{kj} \right)^{\theta_3+1} \Bigg|_{t_{I_j,j}}^{\tau_j} \right] \\
&= \frac{\exp(-\theta_1)}{\tau^{\theta_3+1}(\theta_3+1)} \left[\sum_{i=1}^{I_j} a_{ij}^{\theta_2 - 1} \left(\left(\sum_{k=1}^{i} a_{kj} W_{kj} \right)^{\theta_3+1} - \left(\sum_{k=1}^{i-1} a_{kj} W_{kj} \right)^{\theta_3+1} \right) \right.
\end{aligned}$$

$$+\ a_{(I_j+1)j}^{\theta_2-1}\left(\left(a_{(I_j+1)j}\left(\tau_j-\sum_{k=1}^{I_j}W_{kj}\right)+\sum_{k=1}^{I_j}a_{kj}W_{kj}\right)^{\theta_3+1}-\left(\sum_{k=1}^{I_j}a_{kj}W_{kj}\right)^{\theta_3+1}\right)\Bigg]$$

$$=\frac{\exp(-\theta_1)}{\tau^{\theta_3+1}(\theta_3+1)}\cdot\left[\sum_{i=1}^{I_j+1}a_{ij}^{\theta_2-1}\left(C_j(i)^{\theta_3+1}-C_j(i-1)^{\theta_3+1}\right)\right].$$

The assertion for the load-sharing model with additive damage accumulation follows similarly using

$$\begin{aligned}\int_0^{\tau_j}\lambda_j^A(t)dt&=\int_0^{\tau_j}\frac{1}{\tau}\exp(-\theta_1)\left(a_j(t)+\theta_3\frac{1}{\tau}A_j(t)\right)^{\theta_2}dt\\&=\sum_{i=1}^{I_j}\int_{t_{i-1,j}}^{t_{i,j}}\frac{\exp(-\theta_1)}{\tau}\left(a_{ij}+\theta_3\frac{1}{\tau}A_j(t)\right)^{\theta_2}dt\\&+\int_{t_{I_j,j}}^{\tau_j}\frac{\exp(-\theta_1)}{\tau}\left(a_{(I_j+1)j}+\theta_3\frac{1}{\tau}A_j(t)\right)^{\theta_2}dt.\end{aligned}$$

To calculate the likelihood function, note that $A_j(t_{i,j})=C_j(i)$ holds for $i=1,\ldots,I_j$. Hence, for the load-sharing model with multiplicative damage accumulation, we get

$$\lambda_j^M(t_{i,j})=\frac{1}{\tau}\exp(-\theta_1)a_{ij}^{\theta_2}\left(\frac{1}{\tau}C_j(i)\right)^{\theta_3}$$

and for the load-sharing model with additive damage accumulation, we have

$$\lambda_j^A(t_{i,j})=\frac{1}{\tau}\exp(-\theta_1)\left(a_{ij}+\theta_3\frac{1}{\tau}C_j(i)\right)^{\theta_2}.$$

This completes the proof using form (17) for a likelihood function of a point process and using the fact that the point processes from the J systems are stochastically independent. ■

Proof of Corollary II.2: The intensity function λ_j^W of a load-sharing model without damage accumulation satisfies

$$\begin{aligned}\int_0^{\tau_j}\lambda_j^W(t)dt&=\int_0^{\tau_j}\frac{1}{\tau}\exp(-\theta_1)a_j(t)^{\theta_2}\,dt\\&=\frac{\exp(-\theta_1)}{\tau}\left[\sum_{i=1}^{I_j+1}a_{ij}^{\theta_2}W_{ij}\right]\end{aligned}$$

so that with $\lambda_j^W(t_{i,j})=\frac{1}{\tau}\exp(-\theta_1)a_{ij}^{\theta_2}$ the form of the likelihood function follows from formula (17) for the likelihood function of a general point process.

Hence, $C_j(i)-C_j(i-1)=a_{ij}W_{ij}$ for $i=1,\ldots,I_j+1$, $j=1,\ldots,J$, at once implies the equality $\ln(L_W((\theta_1,\theta_2)^\top))=\ln(L_M((\theta_1,\theta_2,0)^\top))$. The assertion $\ln(L_W((\theta_1,\theta_2)^\top))=\lim_{\theta_3\to 0}\ln(L_A((\theta_1,\theta_2,\theta_3)^\top))$ follows with L'Hospital's rule. ■

Proof of Lemma II.3: The assertion follows from

$$H_{ij}(t|t_{1,j},\ldots,t_{i-1,j})=-\ln(S_{ij}(t|t_{1,j},\ldots,t_{i-1,j}))$$

and the fact that the conditional distribution of $S_{ij}(T_{i,j}|T_{1,j},\ldots,T_{i-1,j})$ given $T_{1,j}=t_{1,j},\ldots,T_{i-1,j}=t_{i-1,j}$ is a uniform distribution on [0,1]. ■

Proof of Theorem II.4: Similarly as in the proof of Theorem II.1, we get for the load-sharing model with multiplicative damage accumulation

$$\begin{aligned}\Lambda_{ij}^M(t)=\int_{t_{i-1,j}}^t\lambda_j^M(u)du&=\frac{\exp(-\theta_1)\,a_{ij}^{\theta_2-1}}{\tau^{\theta_3+1}\,(\theta_3+1)}\\&\cdot\left[(a_{ij}t-a_{ij}t_{i-1,j}+C_j(i-1))^{\theta_3+1}\right.\\&\left.-C_j(i-1)^{\theta_3+1}\right].\end{aligned}$$

This is of the form

$$K(t):=c\,[(at+b)^v-d] \tag{18}$$

which has the following inverse:

$$K^{-t}(y)=\frac{1}{a}\left[\left(\frac{y}{c}+d\right)^{\frac{1}{v}}-b\right]. \tag{19}$$

This implies the form of $(\Lambda_{ij}^M)^{-1}(y)$. The cumulative intensity $\Lambda_{ij}^A(t)$ also is of form (18) so that $(\Lambda_{ij}^A)^{-1}(y)$ is given by (19) as well. ■

Proof of Lemmas III.1 and III.2: Since we combine the proofs for the frequentist case and the Bayesian case, we write $\Pr_\theta(A)=\Pr(A|\Theta=\theta)$ for any set A where Θ is a random variable with realization θ. Set $T:=T_{I_c,0}$ with realization t, $\boldsymbol{\mathcal{N}}_0:=\{\mathcal{N}_j(t)_{t\le\tau_j};j=0,1,\ldots,J\}$ with realization $\mathbf{N}_0$, and $\mathbb{P}(\theta,\boldsymbol{\mathcal{N}}_0):=[q_{\alpha/4}^{\mathcal{M}}(\theta),q_{1-\alpha/4}^{\mathcal{M}}(\theta)]$ the interval of the predictive distribution satisfying

$$\begin{aligned}&\Pr(T\in\mathbb{P}(\Theta,\boldsymbol{\mathcal{N}}_0)|\Theta=\theta,\boldsymbol{\mathcal{N}}_0=\mathbf{N}_0)\\=&\int\mathbb{1}_{\mathbb{P}(\theta,\mathbf{N}_0)}(t)\;p(t|\theta,\mathbf{N}_0)\;dt\ge 1-\frac{\alpha}{2}.\end{aligned} \tag{20}$$

Both prediction intervals $\mathbb{P}_{\mathcal{M},1-\alpha}^F(\boldsymbol{\mathcal{N}}_0)$ and $\mathbb{P}_{\mathcal{M},1-\alpha}^B(\boldsymbol{\mathcal{N}}_0)$ are of the form $\mathbb{P}(\boldsymbol{\mathcal{N}}_0):=\bigcup_{\tilde\theta\in\mathbb{C}(\boldsymbol{\mathcal{N}}_0)}\mathbb{P}(\tilde\theta,\boldsymbol{\mathcal{N}}_0)$ with $\mathbb{C}(\boldsymbol{\mathcal{N}}_0):=\mathbb{C}_{\mathcal{M},1-\alpha/2}^F$ in the frequentist case and $\mathbb{C}(\boldsymbol{\mathcal{N}}_0):=\mathbb{C}_{\mathcal{M},1-\alpha/2}^B$ in the Bayesian case. Then (20) implies

$$\begin{aligned}&Pr(T\notin\mathbb{P}(\boldsymbol{\mathcal{N}}_0)|\Theta=\theta)\\&=Pr\left(T\notin\bigcup_{\tilde\theta\in\mathbb{C}(\boldsymbol{\mathcal{N}}_0)}\mathbb{P}(\tilde\theta,\boldsymbol{\mathcal{N}}_0)\middle|\Theta=\theta\right)\\&=Pr\left(T\notin\bigcup_{\tilde\theta\in\mathbb{C}(\boldsymbol{\mathcal{N}}_0)}\mathbb{P}(\tilde\theta,\boldsymbol{\mathcal{N}}_0),\theta\in\mathbb{C}(\boldsymbol{\mathcal{N}}_0)\middle|\Theta=\theta\right)\\&+\ Pr\left(T\notin\bigcup_{\tilde\theta\in\mathbb{C}(\boldsymbol{\mathcal{N}}_0)}\mathbb{P}(\tilde\theta,\boldsymbol{\mathcal{N}}_0),\theta\notin\mathbb{C}(\boldsymbol{\mathcal{N}}_0)\middle|\Theta=\theta\right)\end{aligned}$$

$$\begin{aligned}
&\leq Pr\ (T \notin \mathbb{P}(\theta, \boldsymbol{\mathcal{N}}_0)|\ \Theta = \theta) + Pr\ (\theta \notin \mathbb{C}(\boldsymbol{\mathcal{N}}_0)|\ \Theta = \theta) \\
&= \int Pr\,(T \notin \mathbb{P}(\theta, \mathbf{N}_0)|\Theta = \theta, \boldsymbol{\mathcal{N}}_0 = \mathbf{N}_0)\ \ p(\mathbf{N}_0|\theta)\ d\mathbf{N}_0 \\
&+\ \Pr\ (\theta \notin \mathbb{C}(\boldsymbol{\mathcal{N}}_0)|\ \Theta = \theta) \\
&\leq \frac{\alpha}{2} + Pr\ (\theta \notin \mathbb{C}(\boldsymbol{\mathcal{N}}_0)|\ \Theta = \theta)\,. \qquad (21)
\end{aligned}$$

In the frequentist case, $\mathbb{C}(\boldsymbol{\mathcal{N}}_0)$ is an asymptotic $(1-\frac{\alpha}{2})$-confidence set satisfying $\lim_{J\to\infty} \Pr(\theta \notin \mathbb{C}(\boldsymbol{\mathcal{N}}_0)|\Theta = \theta) \leq \frac{\alpha}{2}$ so that the assertion of Lemma III.1 follows.

In the Bayesian case, $\mathbb{C}(\boldsymbol{\mathcal{N}}_0)$ is a $(1-\frac{\alpha}{2})$ credible set satisfying

$$\int \mathbb{1}_{\mathbb{C}(\mathbf{N}_0)}(\theta)\ p(\theta|\mathbf{N}_0)\ d\theta \geq 1 - \frac{\alpha}{2}$$

so that (21) implies

$$\begin{aligned}
&Pr(T \notin \mathbb{P}(\boldsymbol{\mathcal{N}}_0)) = \int \Pr(T \notin \mathbb{P}(\boldsymbol{\mathcal{N}}_0)|\Theta = \theta)\ p(\theta)\ d\theta \\
&\leq\ \frac{\alpha}{2} + 1 - \int \Pr\,(\theta \in \mathbb{C}(\boldsymbol{\mathcal{N}}_0)|\ \Theta = \theta)\ \ p(\theta)\ d\theta \\
&=\ \frac{\alpha}{2} + 1 - \int\int \mathbb{1}_{\mathbb{C}(\mathbf{N}_0)}(\theta)\ p(\mathbf{N}_0|\theta)\ d\mathbf{N}_0\ p(\theta)\ d\theta \\
&=\ \frac{\alpha}{2} + 1 - \int\int \mathbb{1}_{\mathbb{C}(\mathbf{N}_0)}(\theta)\ \ p(\theta|\mathbf{N}_0)\ d\theta\ p(\mathbf{N}_0)\ d\mathbf{N}_0.
\end{aligned}$$

Hence, the assertion of Lemma III.2 follows as well. ■

ACKNOWLEDGMENT

The authors would like to thank the reviewers for their helpful comments which improved the article.

REFERENCES

[1] P. H. Kvam and E. A. Peña, "Estimating load-sharing properties in a dynamic reliability system," *J. Am Statist. Assoc.*, vol. 100, no. 469, pp. 262–272, 2005.

[2] D. G. Harlow and S. L. Phoenix, "Probability distributions for the strength of fibrous materials under local load sharing I: Two-level failure and edge effects," *Adv. Appl. Probability*, vol. 14, no. 1, pp. 68–94, 1982.

[3] L. Tierney, "Asymptotic bounds on the time to fatigue failure of bundles of fibers under local load sharing," *Adv. Appl. Probability*, vol. 14, no. 1, pp. 95–121, 1982. [Online]. Available: http://www.jstor.org/stable/1426735

[4] R. L. Smith, "The asymptotic distribution of the strength of a series-parallel system with equal load-sharing," *Ann. Probability*, vol. 10, no. 1, pp. 137–171, 1982. [Online]. Available: http://www.jstor.org/stable/2243777

[5] R. L. Smith, "Limit theorems and approximations for the reliability of load-sharing systems," *Adv. Appl. Probability*, vol. 15, no. 2, pp. 304–330, 1983. [Online]. Available: http://www.jstor.org/stable/1426438

[6] S. Lee, S. Durham, and J. Lynch, "On the calculation of the reliability of general load sharing systems," *J. Appl. Probability*, vol. 32, no. 3, pp. 777–792, 1995. [Online]. Available: http://www.jstor.org/stable/3215129

[7] S. L. Phoenix and W. I. Newman, "Time-dependent fiber bundles with local load sharing. II. General Weibull fibers," *Phys. Rev. E*, vol. 80, Dec. 2009, Art. no. 066115.

[8] S. Li and J. Lynch, "On a threshold representation for complex load-sharing systems," *J. Stat. Plan. Inference*, vol. 141, no. 8, pp. 2811–2823, 2011. [Online]. Available: http://www.sciencedirect.com/science/article/pii/S0378375811001030

[9] F. L. Spizzichino, "Reliability, signature, and relative quality functions of systems under time-homogeneous load-sharing models," *Appl. Stochastic Models Bus. Ind.*, vol. 35, no. 2, pp. 158–176, 2019. [Online]. Available: https://onlinelibrary.wiley.com/doi/abs/10.1002/asmb.2397

[10] J. Xu, M. Xie, and Q. Hu, "Reliability assessment for load-sharing systems with exponential components using statistical expansion as a correction," *Appl. Stochastic Models Bus. Ind.*, vol. 35, no. 4, pp. 998–1010, 2019.

[11] J. Zhang, Y. Zhao, and X. Ma, "Reliability modeling methods for load-sharing k-out-of-n system subject to discrete external load," *Rel. Eng. System Saf.*, vol. 193, 2020, Art. no. 106603. [Online]. Available: http://www.sciencedirect.com/science/article/pii/S0951832019302145

[12] H. Kim and P. H. Kvam, "Reliability estimation based on system data with an unknown load share rule," *Lifetime Data Anal.*, vol. 10, no. 1, pp. 83–94, 2004. [Online]. Available: http://dx.doi.org/10.1023/B:LIDA.0000019257.74138.b6

[13] B. Singh, K. Sharma, and A. Kumar, "A classical and Bayesian estimation of a k-components load-sharing parallel system," *Comput. Statist. Data Anal.*, vol. 52, no. 12, pp. 5175–5185, 2008.

[14] C. Park, "Parameter estimation for the reliability of load-sharing systems," *IIE Trans.*, vol. 42, no. 10, pp. 753–765, 2010. [Online]. Available: https://doi.org/10.1080/07408171003670991

[15] C. Park, "Parameter estimation from load-sharing system data using the expectation-maximization algorithm," *IIE Trans.*, vol. 45, no. 2, pp. 147–163, 2013. [Online]. Available: https://doi.org/10.1080/0740817X.2012.669878

[16] Y. Kong and Z.-S. Ye, "A cumulative-exposure-based algorithm for failure data from a load-sharing system," *IEEE Trans. Rel.*, vol. 65, no. 2, pp. 1001–1013, Jun. 2016.

[17] N. Balakrishnan, E. Beutner, and U. Kamps, "Modeling parameters of a load-sharing system through link functions in sequential order statistics models and associated inference," *IEEE Trans. Rel.*, vol. 60, no. 3, pp. 605–611, Sep. 2011.

[18] Y. Kong and Z. Ye, "Interval estimation for k-out-of-n load-sharing systems," *IISE Trans.*, vol. 49, no. 3, pp. 344–353, 2017. [Online]. Available: https://doi.org/10.1080/0740817X.2016.1217102

[19] K. Leckey, C. H. Müller, S. Szugat, and R. Maurer, "Prediction intervals for load sharing systems in accelerated life testing," *Qual. Rel. Eng. Int.*, vol. 36, no. 6, pp. 1895–1915, 2020.

[20] K. Sobczyk and B. F. Spencer, *Random Fatigue. From Data to Theory*. Cambridge, MA, USA: Academic Press, 1992.

[21] S. J. Bae and P. H. Kvam, "A nonlinear random-coefficients model for degradation testing," *Technometrics*, vol. 46, no. 4, pp. 460–469, 2004. [Online]. Available: http://www.jstor.org/stable/25470894

[22] V. R. B. De Oliveira and E. A. Colosimo, "Comparison of methods to estimate the time-to-failure distribution in degradation tests," *Qual. Rel. Eng. Int.*, vol. 20, no. 4, pp. 363–373, 2004.

[23] M. Sánchez-Silva and G.-A. Klutke, *Reliability and Life-Cycle Analysis of Deteriorating Systems*. Berlin, Germany: Springer, 2016.

[24] W. Kahle, S. Mercier, and C. Paroissin, *Degradation Processes in Reliability*. Hoboken, NJ, USA: Wiley, 2016. [Online]. Available: https://onlinelibrary.wiley.com/doi/abs/10.1002/9781119307488.fmatter

[25] C.-H. Yang, J. V. Zidek, and S. W. K. Wong, "Bayesian analysis of accumulated damage models in lumber reliability," *Technometrics*, vol. 61, no. 2, pp. 233–245, 2019. [Online]. Available: https://doi.org/10.1080/00401706.2018.1512900

[26] Z.-S. Ye, L.-P. Chen, L. C. Tang, and M. Xie, "Accelerated degradation test planning using the inverse Gaussian process," *IEEE Trans. Rel.*, vol. 63, no. 3, pp. 750–763, Sep. 2014.

[27] H. Wang, G.-J. Wang, and F.-J. Duan, "Planning of step-stress accelerated degradation test based on the inverse Gaussian process," *Rel. Eng. Syst. Saf.*, vol. 154, no. C, pp. 97–105, 2016. [Online]. Available: https://ideas.repec.org/a/eee/reensy/v154y2016icp97-105.html

[28] F. Haghighi and S. J. Bae, "Reliability estimation from linear degradation and failure time data with competing risks under a step-stress accelerated degradation test," *IEEE Trans. Rel.*, vol. 64, no. 3, pp. 960–971, Sep. 2015.

[29] W. Nelson, "Accelerated life testing - step-stress models and data analyses," *IEEE Trans. Rel.*, vol. R- 29, no. 2, pp. 103–108, Jun. 1980.

[30] M. Kateri and U. Kamps, "Inference in step-stress models based on failure rates," *Stat. Papers*, vol. 56, pp. 639–660, 2015.

[31] J. V. Deshpande, I. Dewan, and U. V. Naik-Nimbalkar, "A family of distributions to model load sharing systems," *J. Statist. Plann. Inference*, vol. 140, no. 6, pp. 1441–1451, Jun. 2010.

[32] J. Xu, B. Liu, and X. Zhao, "Parameter estimation for load-sharing system subject to Wiener degradation process using the expectation-maximization algorithm," *Qual. Rel. Eng. Int.*, vol. 35, no. 4, pp. 1010–1024, 2019.

[33] Y. Kong and Z. Ye, "A conditional test for the exponential distribution in load-sharing systems," in *Proc. IEEE Int. Conf. Ind. Eng. Eng. Manage.*, Bali, Indonesia, Dec. 04–07, 2016, 2016, pp. 512–515.

[34] D. L. Snyder and M. I. Miller, *Random Point Processes in Time and Space*, 2nd ed. New York, NY, USA.: Springer-Verlag, 1991.

[35] M. Jacobsen, *Point Process Theory and Applications. Marked Point and Piecewise Deterministic Processes*. Basel, Switzerland: Birkhäuser, 2006.

[36] D. J. Daley and D. Vere-Jones, *An Introduction to the Theory of Point Processes. Volume I: Elementary Theory and Methods*. Berlin, Germany: Springer, 2003.

[37] P. K. Andersen, Ø. Borgan, R. D. Gill, and N. Keiding, *Statistical Models Based on Counting Processes*. Berlin, Germany: Springer, 1997.

[38] O. H. Basquin, "The exponential law of endurance tests," *Amer. Soc. Test. Mater. Proc.*, vol. 10, 1910, pp. 625–630.

[39] E. Cinlar, *Introduction to Stochastic Processes*. Englewood Cliffs, NJ, USA: Prentice-Hall, 1975.

[40] R Core Team, *R: A Language and Environment for Statistical Computing*, Vienna, Austria: R Foundation for Statistical Computing, 2019. [Online]. Available: https://www.R-project.org/

[41] S. G. Self and K.-Y. Liang, "Asymptotic properties of maximum likelihood estimators and likelihood ratio tests under nonstandard conditions," *J. Amer. Stat. Assoc.*, vol. 82, no. 398, pp. 605–610, 1987. [Online]. Available: https://www.tandfonline.com/doi/abs/10.1080/01621459.1987.10478472

[42] M. J. Schervish, *Theory of Statistics*. New York, NY, USA: Springer-Verlag, 1995.

[43] M. Plummer, "JAGS: A program for analysis of Bayesian graphical models using Gibbs sampling," in *Proc. 3rd Int. Workshop Distrib. Stat. Computing*, 2003, pp. 1–10.

[44] D. Lunn, C. Jackson, N. Best, A. Thomas, D. Spiegelhalter, The BUGS Book: A Practical Introduction to Bayesian Analysis, New York, NY, USA: Chapman and Hall/CRC, 2013.

[45] D. J. Spiegelhalter, N. G. Best, B. P. Carlin, and A. Van Der Linde, "Bayesian measures of model complexity and fit," *J. Roy. Stat. Society: Ser. B. (Statistical Methodol.)*, vol. 64, no. 4, pp. 583–639, 2002.

[46] J. W. Tukey, "Mathematics and the picturing of data," *Proc. Int. Congr. Math.*, vol. 2, pp. 523–531, 1975.

[47] O. Pokotylo, P. Mozharovskyi, and R. Dyckerhoff, "Depth and depth-based classification with R package ddalpha," *J. Stat. Softw.*, vol. 91, no. 5, pp. 1–46, 2019.

[48] L. Zhu and B. P. Carlin, "Comparing hierarchical models for spatio-temporally misaligned data using the deviance information criterion," *Statist. Med.*, vol. 19, no. 17-18, pp. 2265–2278, 2000.

[49] R. Meyer and J. S. Romeo, "Bayesian semiparametric analysis of recurrent failure time data using copulas," *Biometrical J.*, vol. 57, no. 6, pp. 982–1001, 2015.

[50] Q. Sun, Z.-S. Ye, M. Revie, and L. Walls, "Reliability modeling of infrastructure load-sharing systems with workload adjustment," *IEEE Trans. Rel.*, vol. 68, no. 4, pp. 1283–1295, Dec. 2019.